

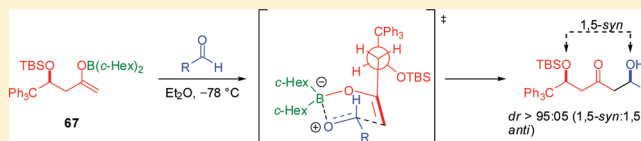
The Role of β -Bulky Substituents in Aldol Reactions of Boron Enolates of Methylketones with Aldehydes: Experimental and Theoretical Studies by DFT Analysis

Luiz C. Dias,* Emílio C. de Lucca, Jr., Marco A. B. Ferreira, Danilo C. Garcia, and Cláudio F. Tormena

Chemistry Institute, State University of Campinas, UNICAMP, 13083-970, C.P. 6154, Campinas, SP, Brazil

S Supporting Information

ABSTRACT: In this work, we show the influence of the volume of the β -substituents on the levels of 1,5-stereoselectivities of aldol reactions of boron enolates generated from β -alkoxy methylketones with aldehydes. Excellent levels of 1,5-*syn* stereoselection were obtained when the β -protecting group is a silicon ether. This remarkable selectivity is attributed to the volume of the β -bulky substituent of the corresponding boron enolate. We have investigated a stereochemical model using DFT analysis to rationalize the sense of 1,5-*syn* stereoselectivities of β -alkyl- β -alkoxy methylketones.



INTRODUCTION

The aldol reaction is a fundamental methodology employed in the construction of carbon–carbon bonds in synthetic organic chemistry. This reaction is useful in the total synthesis of natural products, in particular for the creation of the 1,3-dioxygen relationship in organic molecules with biological and pharmacological significance.¹

The 1,5-remote asymmetric induction in the reaction of boron enolates generated from β -alkoxy methylketones and aldehydes was first observed by Masamune and co-workers in 1989 in their work toward the total synthesis of the C1–C16 fragment of briostatine 1 (Scheme 1).²

In this work, the authors observed that the addition of the boron enolate prepared from methylketone **1** to aldehyde **2** provided the aldol adduct **3** with 1,5-*anti* relationship between the new created stereogenic center and the β -alkoxy group of the boron enolate. This methodology proved to be dependent on the nature of the employed boron reagent. With Et₂BOTf, the authors achieved a 67:33 ratio in favor of the 1,5-*anti* diastereomer. Using the chiral borane **C**, the diastereoselectivity was 86:14 in favor of the 1,5-*anti* aldol adduct, which showed that higher levels of 1,5-*anti* stereocontrol are possible through the reinforcing influence of the boron enolate. Moreover, Masamune and co-workers have demonstrated the difficulties in obtaining good levels of selectivities in favor of the 1,5-*syn* aldol adduct using chiral borane **B**.

The seminal contributions of Paterson³ and Evans,⁴ who independently developed the 1,5-*anti* aldol reaction to a variety of β -alkoxy methylketones, transformed the initial discovery of Masamune in a powerful and synthetically useful aldol methodology widely used in the total synthesis of natural polyketides. From these studies, very high diastereoselectivities (often >20:1) could be obtained from a variety of β -alkoxy methylketones using readily prepared boron enolates. Subsequently, Denmark,⁵ Dias,⁶ and others⁷ have made numerous contributions to advance

our collective understanding of the factors that govern this substrate-controlled stereoselection.

The possible transition states (TS) that lead to the formation of 1,5-*anti* and 1,5-*syn* aldol adducts from aldol reactions of boron enolates of methylketones and aldehydes have been studied by Paton and Goodman.⁸ The authors showed that the aldol reactions of the boron enolates of β -alkoxy methylketones undergo a six-membered cyclic transition state with preference for the boat conformation because the 1,3-diaxial interactions are minimized between one of the ligands of the boron and the ring substituents. They proposed that the β -alkoxy substituent of the enolate is directed into the six-membered ring and participates in a stabilizing H-bond with the aldehyde formyl hydrogen, which leads to further stabilization of the “in” transition state over the “out” transition state (Scheme 2).

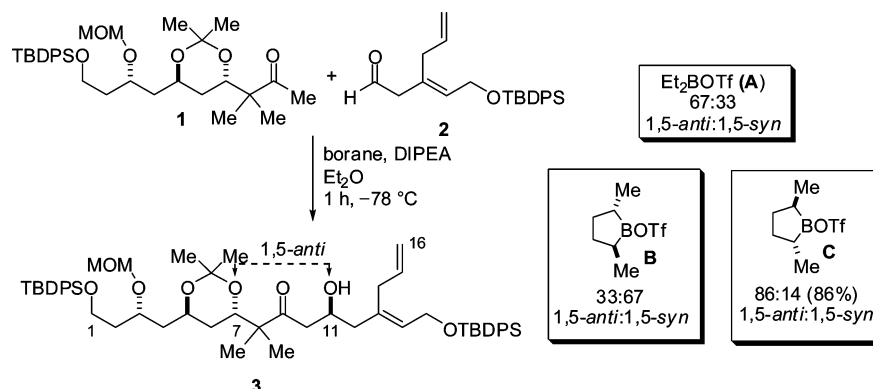
For an alkyl protecting group at the β -oxygen, the high preference for the in-1,5-*anti* transition state over the in-1,5-*syn* is due to the decrease in the steric interactions between the β -alkyl substituent and one of the ligands on boron. However, the in-1,5-*syn* transition states are only slightly lower in energy when compared with the in-1,5-*anti* when silicon ethers are used at the β -position because of the decrease in the steric repulsions between the protecting group and the β -alkyl substituent.

In order to achieve the stereocenter C47 of the C27–C51 fragment of altophyrtin A (spongistatin 1), Paterson and co-workers demonstrated a notable example where the more complex boron enolate **4** overrides the 1,5-*anti* stereoselection typically observed for boron aldol reactions of simple β -alkoxy methylketones, providing the aldol adduct **6** with extraordinary levels of 1,5-*syn* diastereoselectivity (Scheme 3).^{3f} This was the first example that good levels of 1,5-*syn* stereoselection were achieved involving boron enolates of methylketones and was attributed to the more remote stereocenters of the ketone.

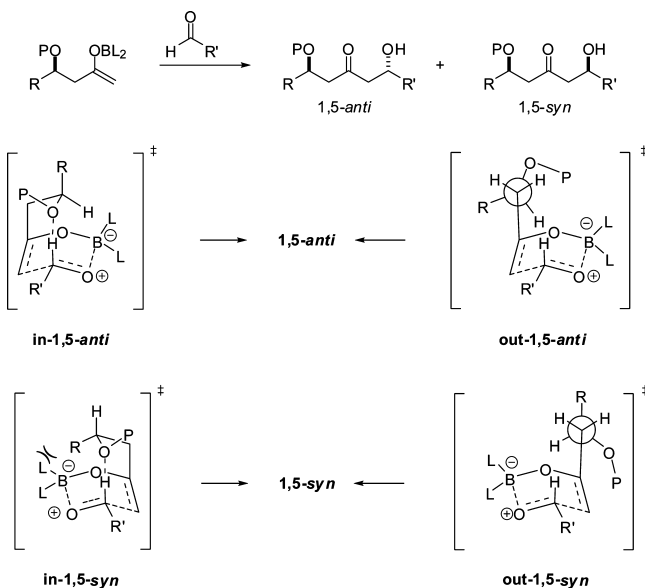
Received: November 10, 2011

Published: January 10, 2012

Scheme 1



Scheme 2



Recently, we demonstrated that good diastereoselectivities in favor of the 1,5-*syn* aldol adducts are possible (Scheme 3).^{6c,d} With both CF₃ and CCl₃ substituents, the 1,5-*syn* remote asymmetric induction occurred independently of the stereo-electronic nature of the β -alkoxy protecting group. Although the best levels of 1,5-*syn* asymmetric induction were obtained with a β -CCl₃ group, these results suggest that the joint action of stereo and electronic character of the β -trihalomethyl groups in the methylketones 7–10 should be the factor responsible for the observed sense of 1,5-*syn* induction.

To understand the stereo and electronic effects of the β -substituents in boron-mediated aldol reactions of β -alkyl- β -alkoxy methylketones, we decided to report an extension of our previous work.⁹ Here, we report our investigation of the influence of 1,5-induction by varying the sizes of the β -alkyl groups (Me, *t*-Bu, *p*-NO₂C₆H₄, Ph₃C) in combination with several protecting groups at the β -oxygen (P = TBS, PMB, Tr, and TPS, triphenylsilyl) 11–19 (Scheme 4).

RESULTS AND DISCUSSION

Preparation of Methylketones 11 and 12. The preparation of methylketone 11 (P = PMB, R = *t*-Bu) and 12 (P = TBS, R = *t*-Bu) began with the preparation of β -hydroxyketone 20. The aldol reaction between acetone and pivalaldehyde,

mediated by L-proline, provided the hydroxyketone 20 in 63% yield and 90% ee, as determined by Mosher ester analysis.¹⁰ The conversion of hydroxyketone 20 into the PMB ether using 4-methoxybenzyl 2,2,2-trichloroacetimidate (PMBTCA) gave the methylketone 11 in 90% yield.¹¹ The protection of the hydroxyl of 20 using TBSCl and imidazole led to the formation of methylketone 12 in 78% yield (Scheme 5).¹²

Aldol Reactions of Boron Enolates of Methylketones 11 and 12. We consequently investigated the aldol reactions between methylketones 11 or 12 and aldehydes 23a–h using (*c*-Hex)₂BCl and Et₃N in Et₂O to generate the kinetic boron enolates (Table 1).

As evident from the results presented in Table 1, for boron enolate 21 (P = PMB, R = *t*-Bu), the aldol adducts 24a–g and 25a–g were obtained in good to excellent yields and with diastereoselectivities on the order of 80:20 in favor of the 1,5-*syn* diastereomer. The levels of selectivity decrease as the steric size of the R group of the aldehyde is increased (entries 1, 4, and 6).

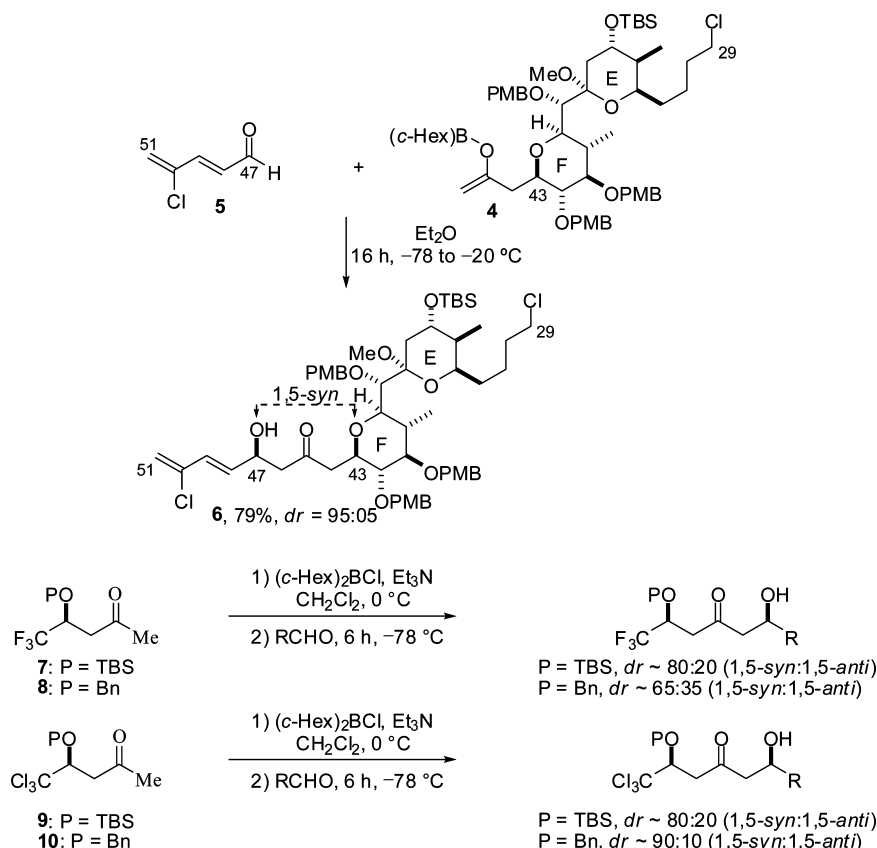
The aldol reactions between the boron enolate 22 (P = TBS, R = *t*-Bu) and aldehydes 23a–h provided the aldol adducts 26a–h and 27a–h in good yields. The diastereoselectivities ranged from 62:38 to 74:26, and the 1,5-*syn* diastereomer is the main observed product. As seen in entries 2, 5, and 7, the diastereoselectivities increase as the steric size of the aldehyde is decreased.

On the basis of these results, we hypothesized that the greatest contribution to the sense of 1,5-*syn* stereoinduction in aldol reactions that involve boron enolates of β -bulky alkyl methylketones is related to the stereo effect of the alkyl substituent at the β -position. However, the electronic effect is not negligible because the sense of 1,5-*syn* induction was lower for enolates 21 (P = PMB, R = *t*-Bu) and 22 (P = TBS, R = *t*-Bu) compared with that for methylketones 10 (P = Bn, R = CCl₃) and 9 (P = TBS, R = CCl₃).

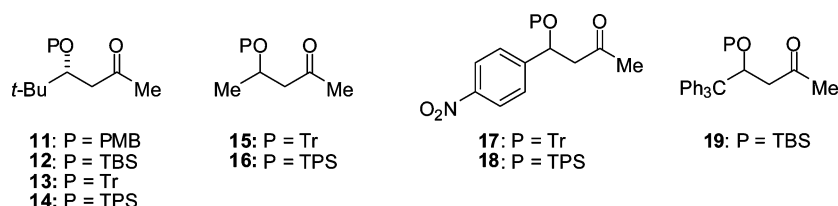
A comparison of the results for methylketone 12 (P = TBS, R = *t*-Bu) with those of previous studies described in the literature reveals a close relationship between the increase in the size of the β -substituent and the increase in the levels of selectivities in favor of the 1,5-*syn* diastereomer (Scheme 6).

The same comparison for methylketone 11 (P = PMB, R = *t*-Bu) in Scheme 7 suggests no change in 1,5-*anti* selectivities when the size of the β -alkyl substituent is varied (entries 1–4). However, with a further increase in the size of the β -substituent (entries 5 and 6), as in this study, we obtained a sharp reversal in selectivity in favor of the 1,5-*syn* aldol adduct.

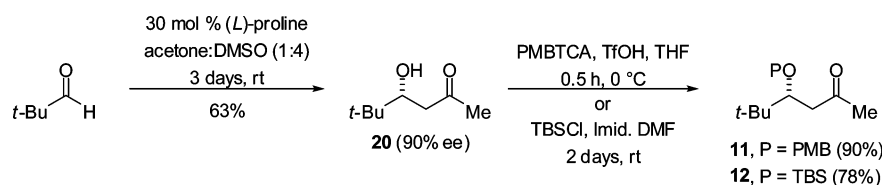
Scheme 3



Scheme 4



Scheme 5



Proof of the Relative Stereochemistry of Aldol Adducts Derived from Methylketones **11 and **12**.** To prove the relative stereochemistry of aldol adducts obtained from methylketone **12** (P = TBS, R = $t\text{-Bu}$) in Table 1, we chose to derivatize the separable mixture of aldol adducts **26c** and **27c** obtained from the aldol reaction between enolate **22** (P = TBS, R = $t\text{-Bu}$) and pivalaldehyde (**23c**) (entry 7, Table 1). A simple analysis of the deviation from the plane of polarized light would be sufficient to determine the relative stereochemistry and hence the absolute stereochemistry. After the TBS protecting group was removed from aldol adduct **26c** (major product), the resulting diol was a *meso* compound, as demonstrated by its lack of optical activity. Nevertheless, the removal

of the TBS group from aldol adduct **27c** (minor product) led to the formation of a diol with a C_2 symmetry axis, a sufficient condition for this compound to be optically active.

The treatment of **26c** with HF in acetonitrile provided the *meso* 1,5-diol **35**. The removal of the TBS group from **27c** generated the C_2 -symmetric 1,5-diol **36**, $[\alpha]_D +50$ (c 0.45, CH_2Cl_2), as required by a 1,5-*anti* relationship (Scheme 8).

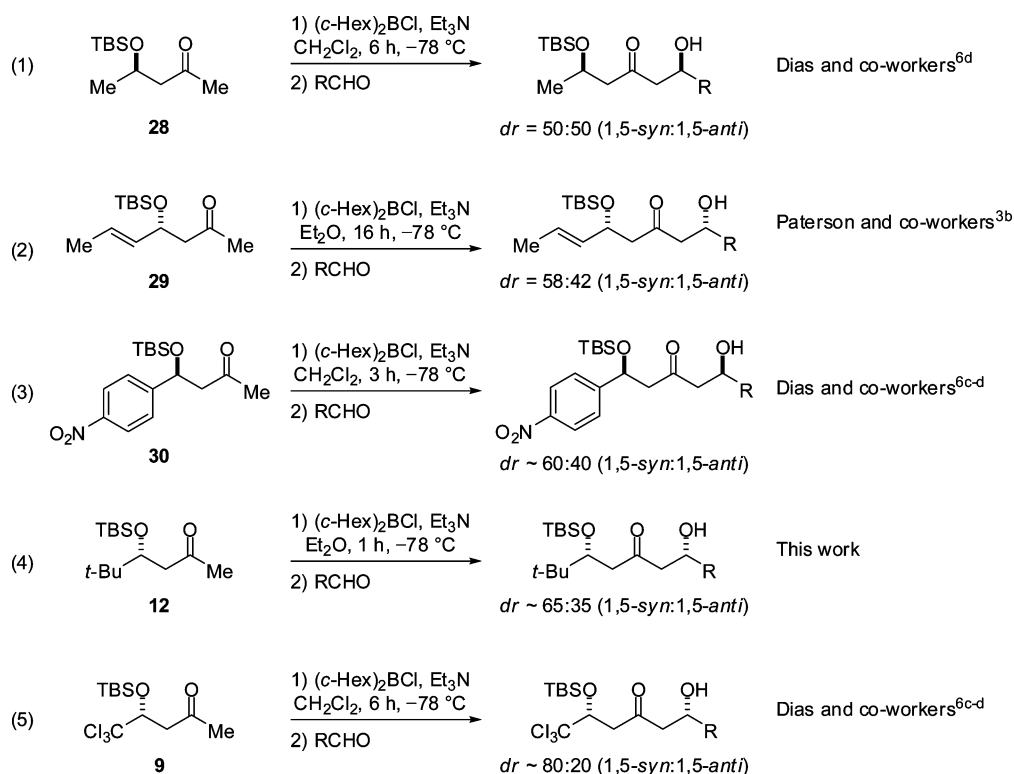
To determine the relative stereochemistry of the aldol adducts obtained from methylketone **11** (P = PMB, R = $t\text{-Bu}$), the 78:22 mixture of **24c** and **25c** (entry 6, Table 1) was treated with DDQ, which provided diols **35** and **36** in 78% yield (Scheme 9).

Table 1. Aldol Reactions of Methylketones 11 and 12

entry	enolate (P)	aldehyde (R) ^a	dr (1,5- <i>syn</i> :1,5- <i>anti</i>) ^b	yield (%) ^c
1	PMB (21)	<i>i</i> -Pr (23a)	80:20	91
2	TBS (22)	<i>i</i> -Pr (23a)	65:35	98
3 ^d	TBS (22)	<i>i</i> -Pr (23a)	65:35	79
4	PMB (21)	Et (23b)	82:18	85
5	TBS (22)	Et (23b)	74:26	92
6	PMB (21)	<i>t</i> -Bu (23c)	78:22	80
7	TBS (22)	<i>t</i> -Bu (23c)	66:34	98
8	PMB (21)	CH ₂ =C(Me) (23d)	81:19	86
9	TBS (22)	CH ₂ =C(Me) (23d)	72:28	86
10	PMB (21)	Ph (23e)	83:17	95
11	TBS (22)	Ph (23e)	68:32	71
12	PMB (21)	<i>p</i> -NO ₂ C ₆ H ₄ (23f)	75:25	85
13	TBS (22)	<i>p</i> -NO ₂ C ₆ H ₄ (23f)	62:38	90
14	PMB (21)	<i>p</i> -OMeC ₆ H ₄ (23g)	79:21	86
15	TBS (22)	<i>p</i> -OMeC ₆ H ₄ (23g)	68:32	86
16	TBS (22)	PhCH ₂ CH ₂ (23h)	65:35	88

^aLiquid aldehydes were added without prior dilution. *p*-Nitrobenzaldehyde (23f) was dissolved in 1.0 mL of CH₂Cl₂. ^bRatio was determined by ¹H and ¹³C NMR analyses of the diastereoisomeric mixture of aldol adducts. ^cIsolated yields of both *syn* and *anti* isomers after SiO₂ gel flash column chromatography. ^dCH₂Cl₂ as solvent. All reactions were quenched by the addition of methanol.

Scheme 6

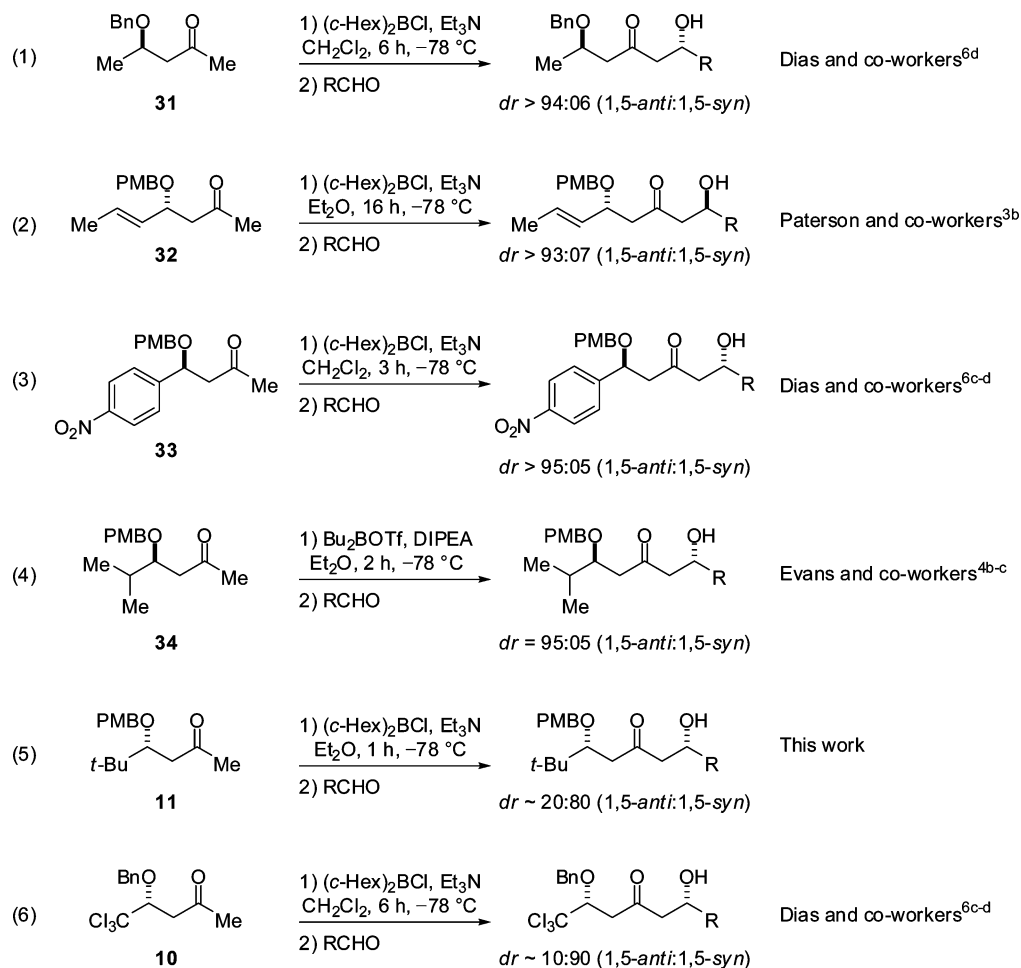


The ¹H and ¹³C NMR spectra of a mixture of diols 35 and 36 prepared by the removal of the PMB protecting group (Scheme 9) were identical with those of diols 35 and 36 obtained by the removal of the TBS protecting group (Scheme 8). We therefore conclude that the diastereomer 1,5-*syn* was also

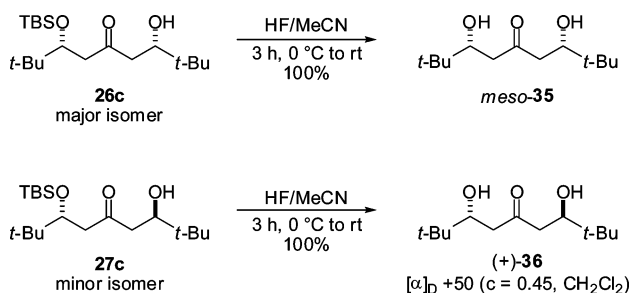
the major product in aldol reactions that involved methylketone 11 (P = PMB, R = *t*-Bu).

Preparation of Methylketones 13, 14, 15, 16, 17, and 18. At this point, we decided to investigate the influence of bulky protecting groups such as triphenylmethyl (Tr, trityl) and

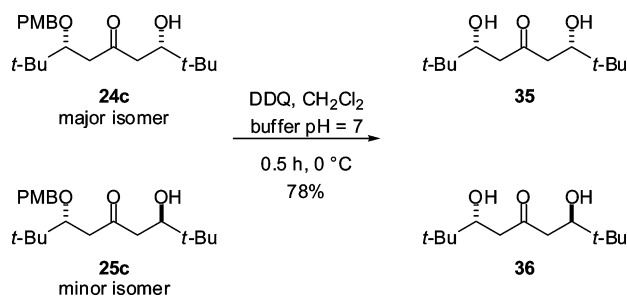
Scheme 7



Scheme 8



Scheme 9



triphenylsilyl (TPS) at the β -oxygen. Protection of compound **20** using TrCl in the presence of AgOTf led to the formation of methylketone **13** (P = Tr, R = *t*-Bu) in 88% yield (Scheme 10).

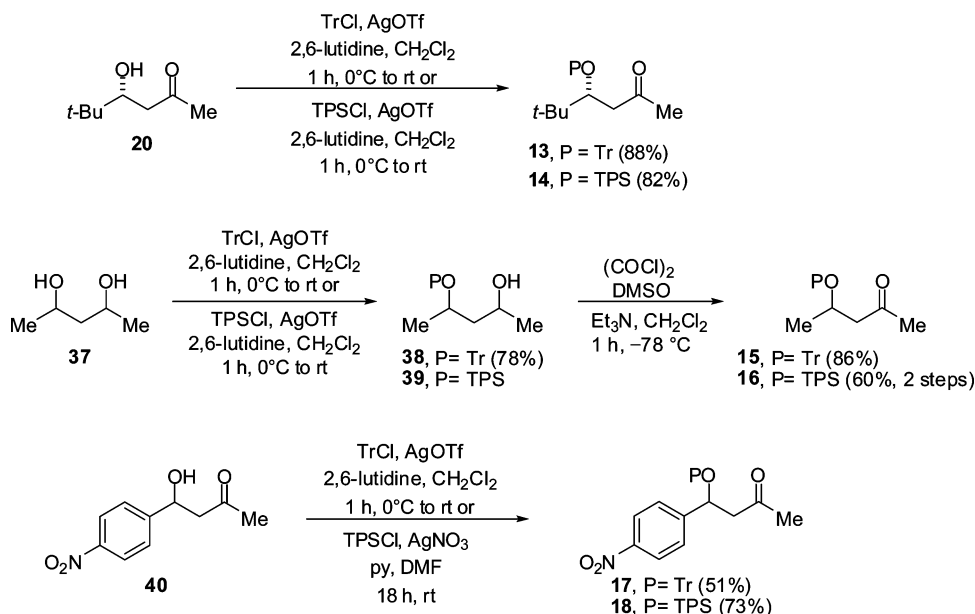
Protection of the hydroxyl group of **20** using TPSCl in the presence of AgOTf led to the formation of methylketone **14** (P = TPS, R = *t*-Bu) in 82% yield.¹³

The preparation of methylketones **15** (P = Tr, R = Me) and **16** (P = TPS, R = Me) was made by a slight modification of the protocol of Lundquist and co-workers,^{13b} using equimolar amounts of diol **37**, AgOTf, and TrCl or TPSCl. Alcohol **38** was thus obtained in 78% yield. The methylketone **15** (P = Tr, R = Me) was obtained in 86% yield by oxidation of alcohol **38** under Swern conditions. Similarly, alcohol **39** was submitted under Swern conditions to provide methylketone **16** (P = TPS, R = Me) in 60% yield (two steps).

Using the same protocol as that used for the preparation of methylketones **13–16**, the treatment of hydroxyketone **40** with AgOTf and TrCl lead to methylketone **17** (P = Tr, R = *p*-NO₂C₆H₄) in 51% yield. In the same way, hydroxyketone **40** was treated with AgNO₃ and TPSCl to provide **18** (P = TPS, R = *p*-NO₂C₆H₄) in 73% yield (Scheme 10).

Aldol Reactions of Boron Enolates of Methylketones 13–18. To examine the influence of larger protecting groups (with different electronic properties), we investigated the aldol reactions that involve boron enolates **41** (P = Tr, R = *t*-Bu), **42** (P = Tr, R = Me), **43** (P = Tr, R = *p*-NO₂C₆H₄), **44** (P = TPS, R = *t*-Bu), **45** (P = TPS, R = Me), and **46** (P = TPS, R = *p*-NO₂C₆H₄) under the same conditions previously employed (Table 2).

Scheme 10



As seen in Table 2, the aldol reactions between the boron enolates **41** (P = Tr, R = *t*-Bu), **42** (P = Tr, R = Me), and **45** (P = TPS, R = Me) with aldehydes provided the corresponding aldol adducts in good yields in an equimolar ratio of the 1,5-*anti* and 1,5-*syn* diastereoisomers. Moreover, the aldol reactions that involved the boron enolate **44** (P = TPS, R = *t*-Bu) with the corresponding aldehydes gave the aldol adducts in good yields and in diastereoselectivities that ranged from 63:37 to 70:30, where the 1,5-*syn* diastereomer was the major product. A clear decrease in the sense of 1,5-*syn* induction was observed when Tr and TPS were employed as protecting groups.

The boron enolates **43** (P = Tr, R = *p*-NO₂C₆H₄) and **46** (P = TPS, R = *p*-NO₂C₆H₄) gave aldol adducts in good yields and, unexpectedly, in 1,5-*anti* selectivity. In previous work,^{6c,d} we showed that aldol reactions that involved methylketone **33** (P = PMB, R = *p*-NO₂C₆H₄) gave aldol adducts in high 1,5-*anti* selectivities, whereas the use of bulkier protecting groups at the β -oxygen, as in methylketone **30** (P = TBS, R = *p*-NO₂C₆H₄), led to poor 1,5-*syn* selectivities.

These results suggest a more complicated relationship between the increased volume of the protecting group and the size of the β -alkyl groups in the 1,5-remote induction.

Proof of the Relative Stereochemistry of Aldol Adducts Derived from Methylketones 14, 17, and 18. To determine the relative stereochemistry of aldol adducts obtained from methylketone **14** (P = TPS, R = *t*-Bu), the mixture of aldol adducts **53c** and **54c** was treated with HF in acetonitrile to provide diols **35** and **36** in quantitative yields (Scheme 11).

The ¹H and ¹³C NMR spectra of the mixture of diols **35** and **36** prepared by the removal of the TPS protecting group (Scheme 11) were identical with those of diols **35** and **36** obtained from the removal of the TBS protecting group (Scheme 8). The major aldol adduct observed in the aldol reactions that involved methylketone **14** (P = TPS, R = *t*-Bu) was also the 1,5-*syn* aldol adduct.

The relative stereochemistries for the aldol adducts obtained from methylketones **17** (P = Tr, R = *p*-NO₂C₆H₄) and **18** (P = TPS, R = *p*-NO₂C₆H₄) were confirmed after the corresponding protecting groups were removed using HF in each

case; the diols **59** and **60** were obtained in a quantitative yields (Scheme 12).

After comparing the previously reported spectroscopic data of diols **59** and **60**,^{6c,d} we concluded that the diastereomers in major proportion in the aldol reactions that involve the methylketone **17** (P = Tr, R = *p*-NO₂C₆H₄) and **18** (P = TPS, R = *p*-NO₂C₆H₄) were 1,5-*anti* aldol adducts.

Preparation of Methylketone 19. As shown in Scheme 6, the aldol reactions that involve boron enolates generated from β -OTBS methylketones show an interesting relationship: an increase in the volume of the β -alkyl substituent leads to an increase in the levels of 1,5-*syn* selectivities. In this context, we decided to prepare methylketone **19** (P = TBS, R = Ph₃C) to confirm the proposed trend.

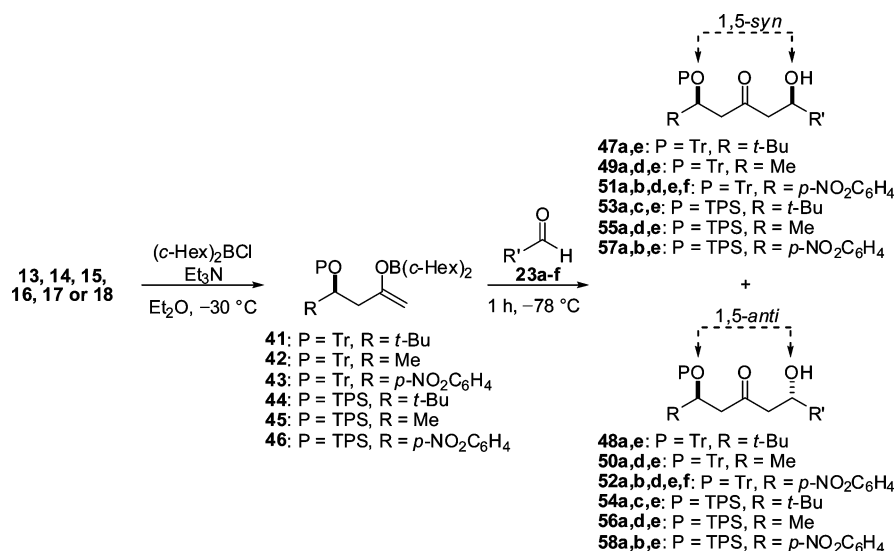
Thus, we first prepared methylketone **19** by reducing the acid **61** with LiAlH₄ to provide alcohol **62** in 69% yield (Scheme 13).¹⁴ Aldehyde **63** was then prepared by oxidation of **62** under Swern conditions in 96% yield.¹⁵ The Weinreb amide **64** was enolized with LDA, followed by the addition of aldehyde **63**, to provide **65** in 99% yield.^{4c} Protection of the hydroxyl group in **65** with TBSOTf gave the silicon ether **66** in 85% yield,¹⁶ which, after reaction with MeLi, provided methylketone **19** in 99% yield.^{6e}

Aldol Reactions of the Boron Enolate of Methylketone 19. We next investigated the aldol reactions involving boron enolate **67** (P = TBS, R = Ph₃C) under the same conditions employed previously (Table 3).

As observed in Table 3, the aldol reactions between the boron enolate **67** (P = TBS, R = Ph₃C) and the corresponding aldehydes led to the formation of aldol adducts **68a–g** and **69a–g** in high 1,5-*syn* selectivities and in good yields. These results clearly show that the steric size of β -bulky substituents in β -alkoxy methylketones plays a major role in the 1,5-*syn* stereochemical sense.

Proof of the Relative Stereochemistry of Aldol Adducts Derived from Methylketone 19. To determine the relative stereochemistry of the aldol adducts obtained from the reactions involving boron enolate **67** (P = TBS, R = Ph₃C), we applied a methodology described by Kishi and co-workers.¹⁷

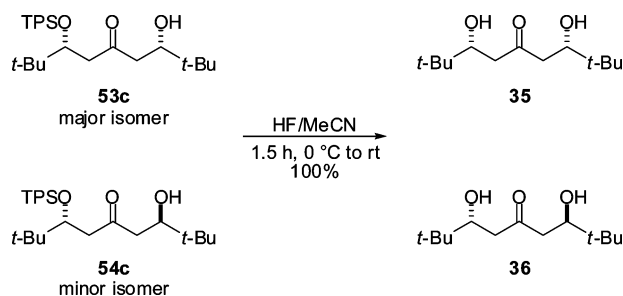
Table 2. Aldol Reactions of Methylketones 13–18



entry	enolate	aldehyde (R') ^a	dr (1,5- <i>syn</i> :1,5- <i>anti</i>) ^b	yield (%) ^c
1	P = Tr, R = <i>t</i> -Bu (41)	<i>i</i> -Pr (23a)	50:50	71
2	P = Tr, R = <i>t</i> -Bu (41)	Ph (23e)	50:50	95
3	P = Tr, R = Me (42)	<i>i</i> -Pr (23a)	50:50	95
4	P = Tr, R = Me (42)	CH ₂ =C(Me) (23d)	50:50	95
5	P = Tr, R = Me (42)	Ph (23e)	50:50	77
6	P = Tr, R = <i>p</i> -NO ₂ C ₆ H ₄ (43)	<i>i</i> -Pr (23a)	27:73	51
7	P = Tr, R = <i>p</i> -NO ₂ C ₆ H ₄ (43)	Et (23b)	40:60	55
8	P = Tr, R = <i>p</i> -NO ₂ C ₆ H ₄ (43)	CH ₂ =C(Me) (23d)	30:70	98
9	P = Tr, R = <i>p</i> -NO ₂ C ₆ H ₄ (43)	Ph (23e)	33:67	76
10	P = Tr, R = <i>p</i> -NO ₂ C ₆ H ₄ (43)	<i>p</i> -NO ₂ C ₆ H ₄ (23f)	30:70	76
11	P = TPS, R = <i>t</i> -Bu (44)	<i>i</i> -Pr (23a)	65:35	88
12	P = TPS, R = <i>t</i> -Bu (44)	<i>t</i> -Bu (23c)	63:37	86
13	P = TPS, R = <i>t</i> -Bu (44)	Ph (23e)	70:30	68
14	P = TPS, R = Me (45)	<i>i</i> -Pr (23a)	50:50	90
15	P = TPS, R = Me (45)	CH ₂ =C(Me) (23d)	50:50	83
16	P = TPS, R = Me (45)	Ph (23e)	50:50	71
17	P = TPS, R = <i>p</i> -NO ₂ C ₆ H ₄ (46)	<i>i</i> -Pr (23a)	39:61	69
18	P = TPS, R = <i>p</i> -NO ₂ C ₆ H ₄ (46)	Et (23b)	33:67	74
19	P = TPS, R = <i>p</i> -NO ₂ C ₆ H ₄ (46)	Ph (23e)	46:54	78

^aLiquid aldehydes were added without prior dilution. *p*-Nitrobenzaldehyde (23f) was dissolved in 1.0 mL of CH₂Cl₂. ^bRatio was determined by ¹H and ¹³C NMR analyses of the diastereoisomeric mixture of aldol adducts. ^cIsolated yields of both *syn* and *anti* isomers after SiO₂ gel flash column chromatography. All reactions were quenched by the addition of methanol.

Scheme 11



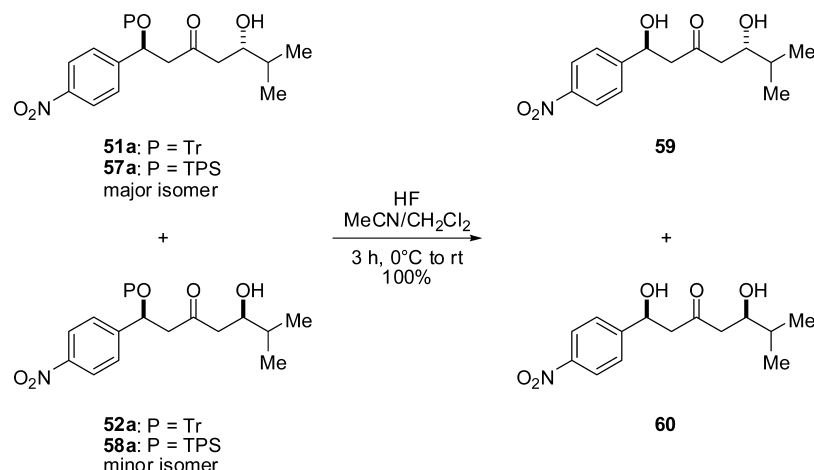
We thus converted the aldol adduct **68b** into two different triols (Scheme 14 and 15). Initially, the aldol adduct **68b** was subjected to 1,3-*syn* carbonyl reduction,¹⁸ which led to the formation of diol **70** in 84% yield and high selectivity (dr > 95:05). The 1,3-*syn* stereochemistry of the secondary alcohols in **70** was determined on the basis of Rychnovsky ¹³C NMR

spectroscopic analysis of the corresponding 1,3-acetonide **71**,¹⁹ which was prepared in 95% yield from diol **70**. The removal of the TBS protecting group from diol **70** with HF in CH₃CN led to the formation of triol **72** in quantitative yield (Scheme 14).

Based on the analysis of the ¹³C NMR spectrum of triol **72** in CD₃OD, the chemical shift value for carbon C3 is 71.8 ppm, which is slightly higher than the shift expected for a *syn/syn* triol (70.7 ppm, according to the Kishi database). However, this value is far from the expected chemical shift for an *anti/syn* triol (68.6 ppm). Therefore, we believe this result confirms the relative stereochemistry for aldol adducts obtained from methylketone **19** (P = TBS, R = Ph₃C) as 1,5-*syn*.

To reinforce this conclusion, we prepared triol **75**. The aldol adduct **68b** was subjected to 1,3-*anti* carbonyl reduction,²⁰ which led to the formation of a mixture of diols **73** and **70** in 50% yield and in 37:63 selectivity that favors the 1,3-*syn* isomer. The relative stereochemistry for the secondary alcohol **73** was determined on the basis of Rychnovsky ¹³C NMR spectroscopic

Scheme 12



Scheme 13

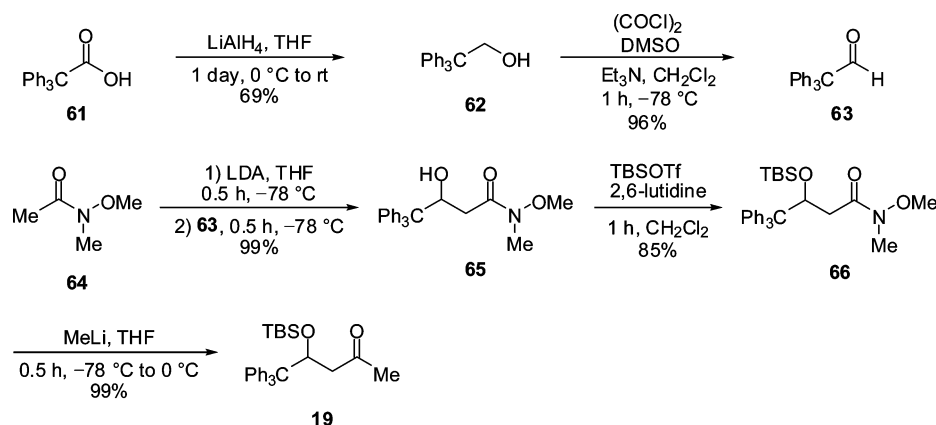
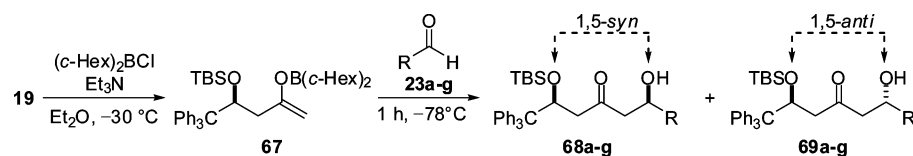


Table 3. Aldol Reactions of Methylketone 19



entry	aldehyde (R) ^a	dr (1,5-syn:1,5-anti) ^b	yield (%) ^c
1	<i>i</i> -Pr (23a)	>95:05	95
2	Et (23b)	>95:05	92
3	<i>t</i> -Bu (23c)	>95:05	98
4	CH ₂ =C(Me) (23d)	>95:05	94
5	Ph (23e)	91:09	89
6	<i>p</i> -NO ₂ C ₆ H ₄ (23f)	>95:05	84
7	<i>p</i> -OMeC ₆ H ₄ (23g)	91:09	78

^aLiquid aldehydes were added without prior dilution. *p*-Nitrobenzaldehyde (**23f**) was dissolved in 1.0 mL of CH₂Cl₂. ^bRatio was determined by ¹H and ¹³C NMR analyses of the diastereoisomeric mixture of aldol adducts. ^cIsolated yields of both *syn* and *anti* isomers after SiO₂ gel flash column chromatography. All reactions were quenched by the addition of methanol.

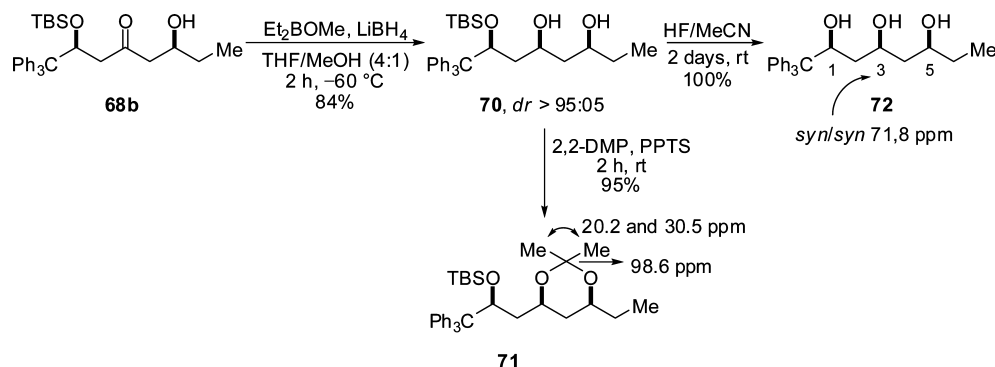
analysis of the corresponding 1,3-acetonide **74** (dr = 37:63),¹⁹ which was prepared in 95% yield from diol **73**. The removal of the TBS protecting group of **73** with HF led to the formation of triol **75** (dr = 37:63) in quantitative yield (Scheme 15).

From the analysis of the ¹³C NMR spectrum of triol **75**, the chemical shift for carbon C3 was 66.7 ppm, which is close to the expected values for *anti/anti* triols according to the Kishi database (66.3 ppm). Thus, we confirmed, unequivocally, that the 1,5-diastereomer obtained in higher proportion in aldol

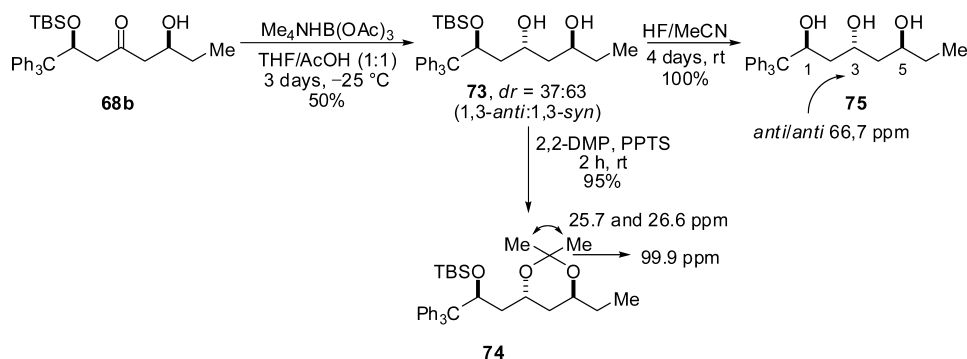
reactions that involved the methylketone **19** (P = TBS, R = Ph₃C) was the 1,5-*syn* aldol adduct.

Rationalization Model. All the boron aldol reactions were conducted under conditions of kinetic control. Because this step is irreversible, the competing boron aldol transition structures in which a new stereocenter is formed allowed us to compare the energies of the aldol transition structures to investigate the effects of β -bulky groups with respect to the 1,5-stereoselectivity.

Scheme 14



Scheme 15



Aldol reactions of β -alkoxy methylketones ($R = CF_3$, CCl_3 , and t -Bu) with TBS or PMB protecting groups and β -bulky alkyl groups showed good 1,5-*syn* selectivities. In addition, a further increase in the steric size of the β -substituent ($R = Ph_3C$) gave only 1,5-*syn* aldol adducts, which reinforced this induction.

On the basis of our experimental results, we conclude that the stereochemical model proposed by Goodman and Paton works only for methylketones with small and medium β -alkyl substituents such as $-Me$, $-CH_2R$, $-i$ -Pr, Ar, etc.

We propose a complementary stereochemical model of induction that includes the volume effect of the β -substituent and the protecting groups at the β -oxygen of β -alkoxy methylketones. In the case of β -bulky substituted methylketones (t -Bu, $-CX_3$, and Ph_3C) with protecting groups of intermediate size such as benzylic ($P = Bn$ and PMB) and silicon ($P = TBS$) derivatives, the relative energies of the “in” transition states that involve formyl H-bonds are higher than those of the “out” transition states because of the steric repulsions $OP \rightleftharpoons R$ for **TS-in-1,5-*anti*** and $L \rightleftharpoons R$ for **TS-in-1,5-*syn***.

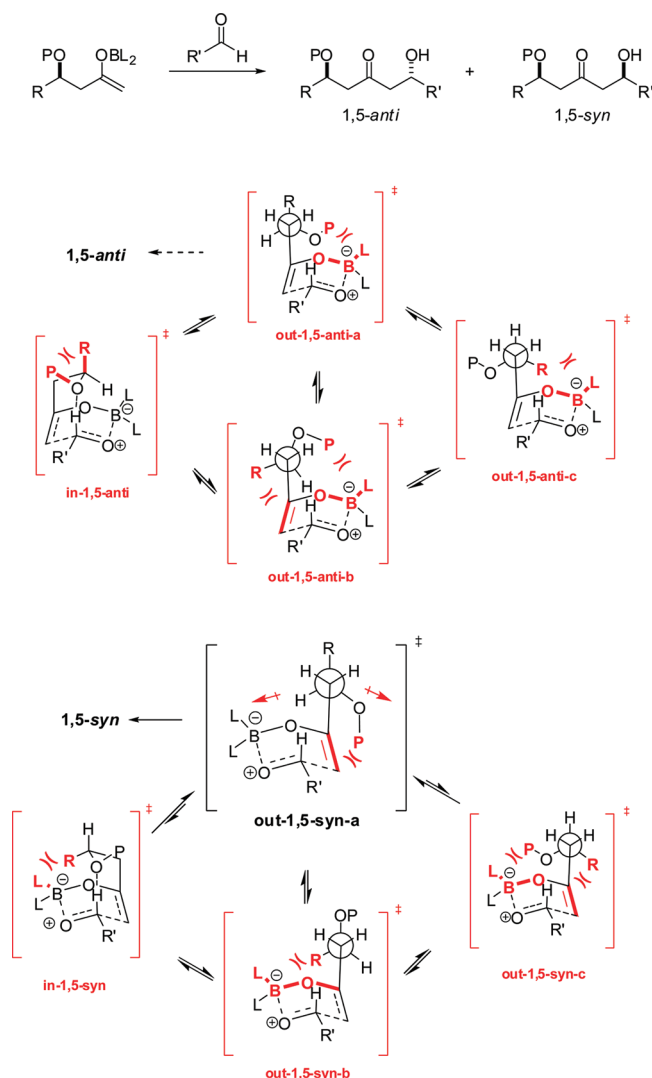
Thus, we postulate that the lower-energy “out” transition state should keep the β -bulky substituent as far as possible from the ring and the ligands of boron. The competitive transition states **TS-out-1,5-*anti*-a** and **TS-out-1,5-*syn*-a** assume this conformation, as depicted in Scheme 16. The orientation of the $-OP$ group in the transition state **TS-out-1,5-*anti*-a** implies greater repulsion with boron ligands and brings together the oxygens of the protecting group and the enolate. Thus, the 1,5-*syn* stereoinduction arises from the transition state **TS-out-1,5-*syn*-a**, which is the lowest-energy transition state; this transition state guides the $-OP$ group in the direction opposite the C–O enolate bond, which partially reduces the steric repulsions and the dipole moment of the system.

However, this sense of induction is lost when larger protecting groups such as Tr (Ph_3C -) and TPS (Ph_3Si -) are employed. In these cases, new repulsive interactions are introduced into the system, which reduces the difference in the relative energies of the competing transition states.

Theoretical calculations involving these systems were made to support the proposed theoretical model and to give support to the conclusions presented.

THEORETICAL ANALYSIS

Computational Methods. Theoretical calculations of the transition states of aldol reactions that involve boron enolates were performed to investigate this reverse substrate-based 1,5-*syn* stereocontrol. All structures were fully optimized through the Gaussian03 or Gaussian09 program.²¹ The 6-31G(d,p) basis sets were applied for this purpose. Single-point calculations (in CH_2Cl_2 or Et_2O) using the default Gaussian09 IEF-PCM²² (UFF radii) or Truhlar SMD²³ solvation models from the optimized gas-phase transition-state geometries were performed to evaluate the relative energies using the B3LYP²⁴ hybrid density functional in combination with the 6-31+G(d,p) basis set.²⁵ The Cartesian coordinates are supplied in the Supporting Information. Paton and Goodman⁸ have observed that the full optimization geometry and energy in solvents are very similar to single-point solvation. We wished to adopt boat-like starting geometries, which have been previously shown by Goodman to be the more favorable conformers. The boat-like transition state prevents 1,3-diaxial-type interactions that occur in the corresponding chairlike transition structures. Frequency calculations ensured that the stationary points represent a maximum on the potential-energy surface, and the corresponding eigenvectors were inspected to confirm the expected aldol reaction coordinates.

Scheme 16. 1,5-Stereochemical Model for β -Bulky-Substituted Methylketones

The natural bond orbital (NBO) energies were calculated at the B3LYP/6-31G(d,p) level using NBO 5.0.²⁶ These delocalization energies were calculated by second-order perturbation theory analysis using the E2PERT=0.05 keyword to reduce the threshold for donor–acceptor delocalization energy interactions from 0.5 kcal mol^{−1} to 0.05 kcal mol^{−1}. We examined the overlap matrix ($S_{<i-j>}$) in the overlap of preorthogonal natural bond orbital (SPNBO) analysis that provided the NBO overlap.

The initial geometries in the diastereoisomeric transition states were generated by rotating the Φ_1 dihedral for “out” conformers, as shown in Scheme 17. Additionally, we generated the “X-in” transition states for the transition states of trihalomethyl methylketones. In the studied models, we replaced the PMB, TBS, and *c*-Hex groups with Bn, TMS, and Me groups, respectively.

β -Trihalomethyl Methylketones. Initially, we investigated the transition states using models for methylketones **9** (P = TBS, R = CCl₃) and **7** (P = TBS, R = CF₃). The initial geometries were generated as shown in Scheme 17. The most significant transition states are shown in Scheme 18 and Table 4 (see Tables S1 and S2 in the Supporting Information for all energies of the observed transition states).

Analysis of the relative energies of the transition states in Table 4 indicated the transition states **out-1,5-syn-a** (0.0 kcal/mol) as being the most stable for methylketones **9** (P = TBS, R = CCl₃) and **7** (P = TBS, R = CF₃), which led to similar relative energies for the two solvation models employed. This result qualitatively predicts the preferential formation of the 1,5-syn aldol adducts, in agreement with our experimental results. We believe that the low energy for the **out-1,5-syn-a** conformer is due to the β -trihalomethyl and β -OTMS substituents being directed as far from the ring as possible.

In addition, the “in” transition states of methylketones **7** and **9** were found to have greater energies than the **out-1,5-syn-a** transition states. The NBO analysis showed small energy values (all below 1 kcal/mol) for the H-bonds between the lone pairs of the β -oxygen (LP_{O1} and LP_{O2}) and the C–H formyl (σ^*_{C-H}) in the “in” transition states. These values are closely related with conformational restrictions imposed by strong repulsions between OP \rightleftharpoons R and L \rightleftharpoons R for the **in-1,5-anti** and **in-1,5-syn** transition states, respectively. The long lengths of the H-bonds (r_{O-HC}), which range from 2.6 to 2.8 Å, and the low values of the matrix overlap $S_{<O-HC>}$ result in the low H-bond energies (for reference, we have included in Supporting Information, section S3, the r_{O-HC} and $S_{<O-HC>}$ values for the competitive transition states of methylketone **34**). Surprisingly, the “in-syn” transition states exhibited H-bonds between the lone pairs of F and Cl atoms and the C–H formyl (σ^*_{C-H}) in the range of 1–2 kcal/mol, which is greater than the energies of the previously discussed oxygen H-bonds. However, this additional stabilization is not sufficient to offset the strong β -CX₃ \rightleftharpoons B–L repulsions responsible for the high energy of these conformers.

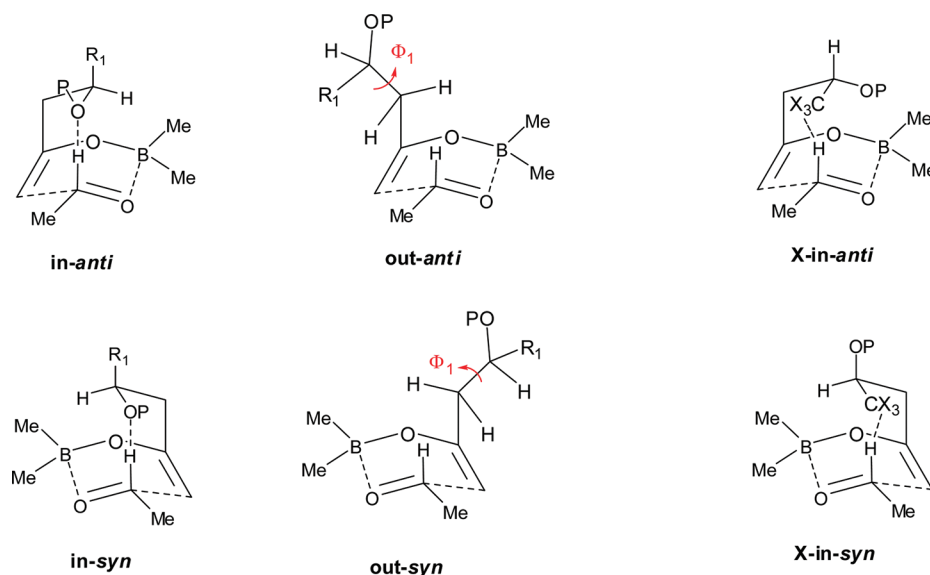
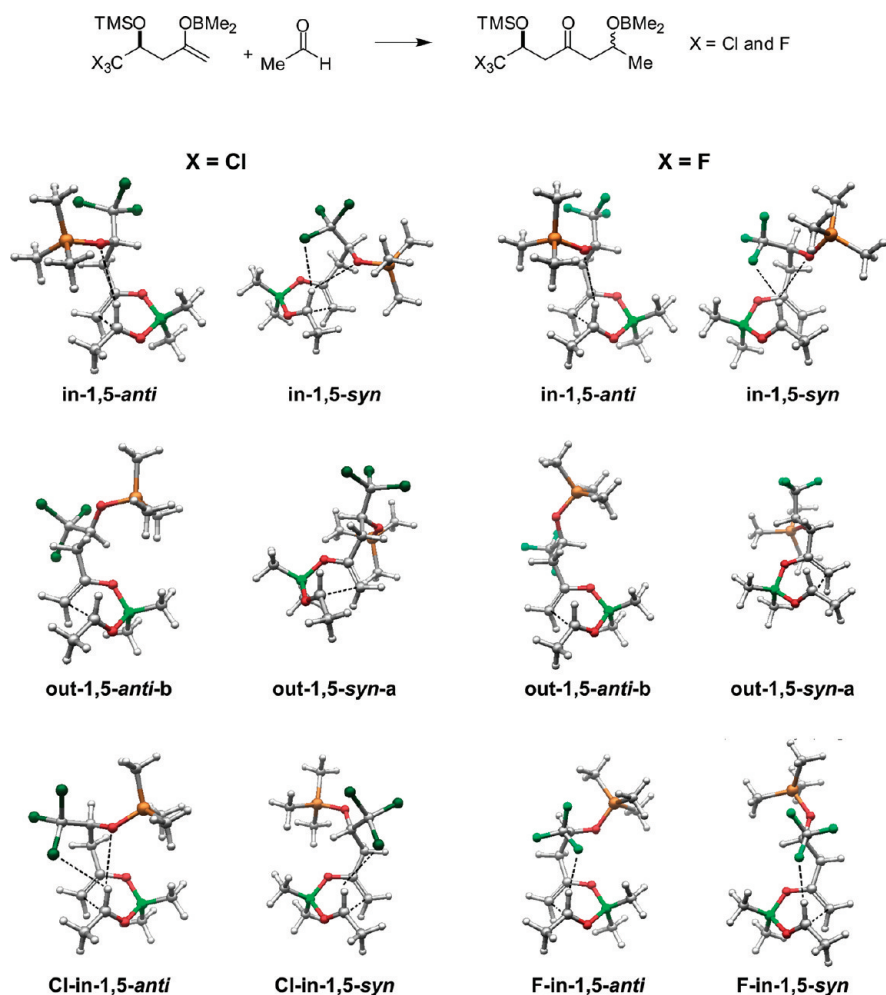
The “X-in” transition states were also characterized. In these cases, despite the stabilization of the X–HC H-bonds (in the range of 1.6–3.4 kcal/mol), the CX₃-oriented groups on the ring increase the relative energy of these conformers.

The next step was to investigate the transition states using models for methylketones **10** (P = Bn, R = CCl₃) and **8** (P = Bn, R = CF₃). The results are shown in Scheme 19 and Table 5 (the energies of all characterized conformers can be found in Tables S4 and S5 in the Supporting Information).

Analysis of the characterized transition states for methylketone **10** (P = Bn, R = CCl₃) indicated that the **out-1,5-syn-a** conformers had the lowest relative energy (0.0 kcal/mol), irrespective of the employed solvation model. The **out-1,5-syn-a** transition states led to preferential formation of the 1,5-syn aldol adducts, in agreement with our experimental results.

In the case of methylketone **8** (P = Bn, R = CF₃), the experimental results were dr \sim 65:35 (1,5-syn:1,5-anti).^{6d} Because of these results, competitive transition states with highly similar relative energies are expected. As depicted in Table 5 (X = F), with the IEF-PCM solvation method, the relative energies for the competitive transition states **in-1,5-anti-b** (0.0 kcal/mol) and **out-1,5-syn-a** (0.3 kcal/mol) are in disagreement with our experimental results. We believe this difference is associated with a deficiency in the IEF-PCM model for predicting the theoretical solvation energy for polyfluorinated molecules.²⁷ However, an inversion in the relative stabilities was observed when the solvation model developed by Truhlar (SMD) was applied. This model significantly improved the solvation energy calculation, and the **out-1,5-syn-a** (0.0 kcal/mol) transition state became more stable than the **in-1,5-anti-b** (0.4 kcal/mol) transition state.

Scheme 17

Scheme 18. Aldol Transition Structures of β -Trihalomethyl- β -Trimethylsilyloxy Dimethyl Boron Enolate and Ethanal

The results described in Table 5 support our model (Scheme 16). Moreover, similar to methylketones 7 and 9 ($\text{P} = \text{TBS}$), methylketones 8 and 10 ($\text{P} = \text{PMB}$) had “in” transition-state energies higher than those of **out-1,5-syn-a**, as well as low H-bond ($\text{O}-\text{HC}$) energies that ranged from 0.78 to 1.8 kcal/mol.

This result is interesting because β -OBn methylketones have traditionally been associated with high 1,5-*anti* selectivities precisely because of the stabilization that arises from the H-bonds ($\text{O}-\text{HC}$). However, the conformational constraints in our system in the “in” transition states impose strong

Table 4. Aldol Transition Structures Calculated at B3LYP and with Basis Set 6-31G(d,p), the SCRf in B3LYP/6-31+G(d,p) and IEF-PCM (UFF Radii) or SMD Solvation Models, and the Delocalization Energies and NBO Overlap Matrix (S) of the Stabilizing H-Bond

TS	IEF-PCM $E_{\text{rel}}(\text{CH}_2\text{Cl}_2)$ (kcal/mol)	SMD $E_{\text{rel}}(\text{CH}_2\text{Cl}_2)$ (kcal/mol)	r (Å)	E_{NBO} (kcal/mol)	ΣE_{NBO} (kcal/mol)	$S_{<\text{X}-\text{H}\cdots\text{C}>}$
X = Cl	in-1,5- <i>anti</i>	4.4	$r_{\text{O}-\text{HC}} = 2.85$	$\text{LP}_{\text{O}2} = 0.26$	0.26	0.061
				$\text{LP}_{\text{O}1} = 0.27$		
	Cl-in-1,5- <i>anti</i>	6.6	$r_{\text{Cl}-\text{HC}} = 2.90$	$\text{LP}_{\text{Cl}2} = 0.49$	0.83	0.067 0.023
				$\text{LP}_{\text{Cl}3} = 0.07$		
	out-1,5- <i>anti-b</i>	1.9	-	-	-	-
	in-1,5- <i>syn</i>	6.4	$r_{\text{O}-\text{HC}} = 2.94$ $r_{\text{Cl}-\text{HC}} = 2.79$	$\text{LP}_{\text{O}1} = 0.18$	2.4	0.047 0.13
				$\text{LP}_{\text{Cl}1} = 0.21$ $\text{LP}_{\text{Cl}2} = 2.02$		
	Cl-in-1,5- <i>syn</i>	1.9	$r_{\text{Cl}-\text{HC}} = 2.91$	$\text{LP}_{\text{Cl}1} = 0.14$	1.6	0.038 0.083 0.063
				$\text{LP}_{\text{Cl}2} = 0.87$ $\text{LP}_{\text{Cl}3} = 0.55$		
	out-1,5- <i>syn-a</i>	0.0	-	-	-	-
X = F	in-1,5- <i>anti</i>	3.2	$r_{\text{O}-\text{HC}} = 2.61$	$\text{LP}_{\text{O}1} = 0.47$	0.99	0.075 0.070
				$\text{LP}_{\text{O}2} = 0.52$		
	F-in-1,5- <i>anti</i>	5.7	$r_{\text{F}-\text{HC}} = 2.21$	$\text{LP}_{\text{F}1} = 0.14$	1.6	0.096 0.019 0.10
				$\text{LP}_{\text{F}2} = 0.87$ $\text{LP}_{\text{F}3} = 0.55$		
	out-1,5- <i>anti-b</i>	0.8	-	-	-	-
	in-1,5- <i>syn</i>	3.8	$r_{\text{O}-\text{HC}} = 2.76$ $r_{\text{F}-\text{HC}} = 2.37$	$\text{LP}_{\text{O}1} = 0.29$	1.4	0.06 -0.035
				$\text{LP}_{\text{O}2} = 0.13$ $\text{LP}_{\text{F}1} = 0.14$ $\text{LP}_{\text{F}2} = 0.87$		
	F-in-1,5- <i>syn</i>	1.9	$r_{\text{F}-\text{HC}} = 2.20$	$\text{LP}_{\text{F}1} = 1.90$	3.4	0.11 0.051 0.066
				$\text{LP}_{\text{F}2} = 0.55$ $\text{LP}_{\text{F}3} = 0.99$		
	out-1,5- <i>syn-a</i>	0.0	-	-	-	-

repulsions between $\beta\text{-OBn} \rightleftharpoons \beta\text{-CX}_3$ and $\text{L} \rightleftharpoons \beta\text{-CX}_3$, which leads to greater H-bond ($r_{\text{O}-\text{HC}}$) distances, in the range of 2.5–2.7 Å, and low matrix overlap $S_{<\text{O}-\text{H}\cdots\text{C}>}$ values. Moreover, despite the high energy associated with the stabilizing halogen H-bond ($\text{X}-\text{HC}$) (1.2–4.5 kcal/mol), the “X-in” transition states had high relative energies because of the orientation of the $\beta\text{-CX}_3$ groups on the ring.

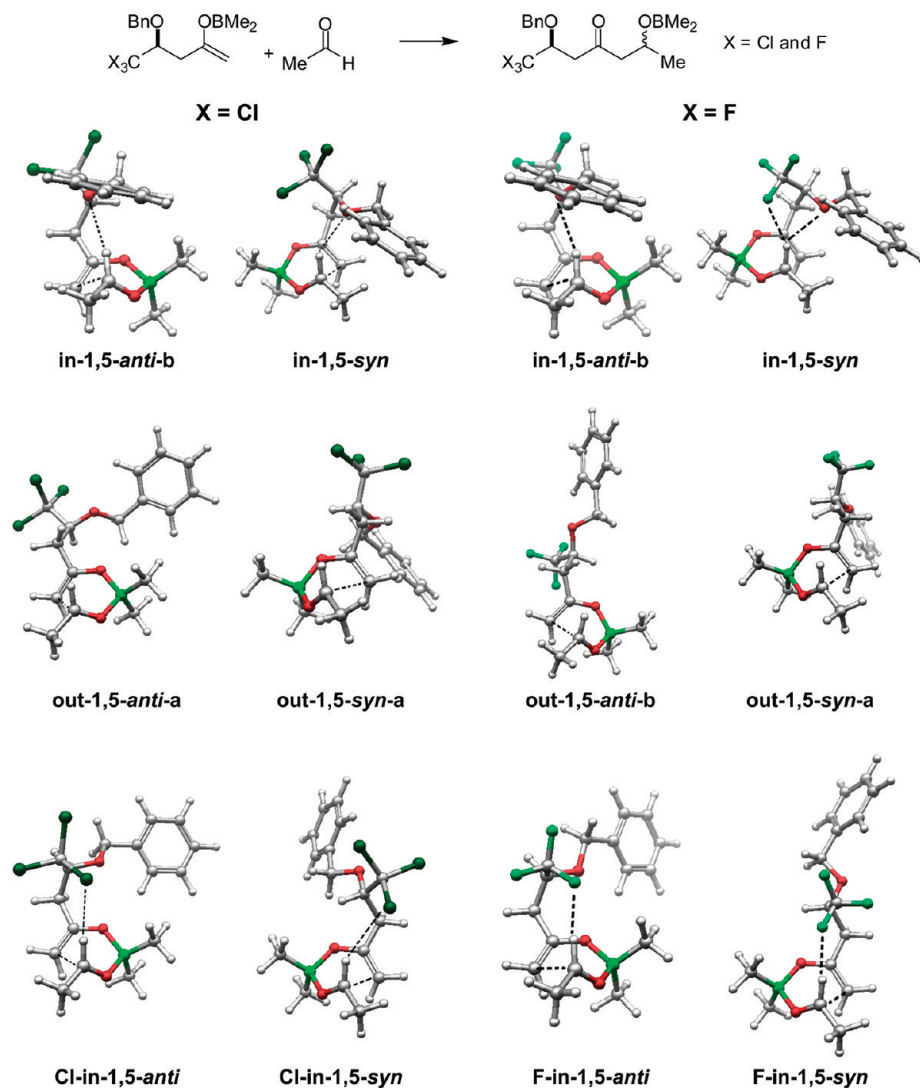
β -tert-Butyl Methylketones and β -Triphenylmethyl Methylketones. We hypothesized that the 1,5-*syn* selectivity would arise from the stereo effect of β -bulky substituents based on the results obtained with the methylketones **11** ($\text{P} = \text{PMB}$, $\text{R} = t\text{-Bu}$) and **12** ($\text{P} = \text{TBS}$, $\text{R} = t\text{-Bu}$) (Table 1). This stereo effect led to 1,5-*syn* selectivities similar to those obtained using methylketones **9** ($\text{P} = \text{TBS}$, $\text{R} = \text{CCl}_3$) and **10** ($\text{P} = \text{Bn}$, $\text{R} = \text{CCl}_3$). We continued our theoretical study using models for methylketones **11** and **12** as represented in Scheme 20 and Table 6 (Tables S7 and S8 in the Supporting Information describe the energies of all the characterized transition states).

According to Table 6, the out-1,5-*syn-a* conformers for methylketones **11** and **12** showed the lowest relative energies (~1 kcal/mol more stable than out-1,5-*anti-b*), which predicts the 1,5-*syn* selectivity of the aldol adducts. These results agree perfectly with our model (Scheme 16) and are related to steric minimization between the β -*t*-Bu and β -OP groups and the ring and the boron ligands. The high energy of the “in” transition states arise from the severe repulsions between the $\text{OP} \rightleftharpoons t\text{-Bu}$ and $\text{L} \rightleftharpoons t\text{-Bu}$ groups in the in-1,5-*anti* and in-1,5-*syn*

transition states. For the “in” conformers, the long lengths of the H-bonds ($r_{\text{O}-\text{HC}}$), which are in the range of 2.7 to 3.0 Å, and the low matrix overlap $S_{<\text{O}-\text{H}\cdots\text{C}>}$ values lead to low H-bond energies that range from 0.16 to 0.54 kcal/mol.

For the study of methylketone **19** ($\text{P} = \text{TBS}$, $\text{R} = \text{Ph}_3\text{C}$), we considered all six conformers related to the C–Ph and C–C sigma-bond rotations of the trityl protecting group (see the Supporting Information, section S9, for further details). The structures with the lowest energies are shown in Scheme 21 and Table 7 (for visualization of all characterized structures see Supporting Information, Table S8).

As shown in Table 7, the large gap between the competitive transition states out-1,5-*syn-a-i* (0.0 kcal/mol) and out-1,5-*anti-a-v* (3.4 and 3.6 kcal/mol for IEF-PCM and SMD solvation models, respectively) suggests the exclusive formation of the 1,5-*syn* aldol adduct, which is consistent with the experimental diastereoselectivity ($\text{dr} > 95:05$, 1,5-*syn*:1,5-*anti*). The energy difference between the competitive transition states of all other aldol reactions studied in this work are in the range of 0.4–1.7 kcal/mol and in low-to-moderate experimental 1,5-*syn* selectivities. Thus, the proposed induction model (Scheme 16) helps explain the high 1,5-*syn* selectivity obtained, which occurred via the lowest-energy conformer out-1,5-*syn-a-i*. This conformer minimizes the steric repulsions between the $\beta\text{-Ph}_3\text{C}$ and $\beta\text{-OTMS}$ groups and the ring and the boron ligands. Therefore, our expectation was that a higher selectivity would be achieved when a bulkier β -group, such as $\beta\text{-Ph}_3\text{C}$, was

Scheme 19. Aldol Transition Structures of β -Trihalomethyl- β -Benzyloxy Dimethyl Boron Enolate and Ethanal

employed. Interestingly, the volume of the β - Ph_3C group strongly intervened in the “in” transition states via the severe $\text{OP} \rightleftharpoons \beta$ - Ph_3C repulsion because $\text{TS-in-1,5-anti-iii}$ (6 kcal/mol more energetic than out-1,5-syn-a-i) showed no H-bonds ($r_{\text{O-HC}}$ of 3.45 Å). In addition, the severe repulsion between the $\text{L} \rightleftharpoons \beta$ - Ph_3C groups prevented the formation of the in-1,5-syn transition state, which could not be characterized.

Role of Oxygen Steric Repulsion in β -Bulky Methylketones. As previously discussed, the bulky β -group orients itself as far as possible from the ring in the transition states. Therefore, independent of the conventional protecting groups such as TBS and PMB, the out-1,5-syn-a conformers possess the lowest energy. However, the TS-out-1,5-anti-a conformers also satisfy this condition (Figure 1). Moreover, steric repulsions involving the protecting groups are present in both conformations.

As is evident in the graphic in the Figure 1, the TS-out-1,5-anti-a conformers were between 1.7 and 3.6 kcal/mol higher in energy than the out-1,5-syn-a conformers. This large energy difference is attributed to the interaction between the enolate bond (C–O) and the β -oxygen. The conformer out-1,5-syn-a drives the β -OP group in the opposite direction from the

C–O enolate bond, which leads to a strong minimization of the dipole moment and steric repulsion in the system.²⁸

β -Triphenylmethoxy Methylketones. According to the data presented in Table 2, the sense of 1,5-syn induction of β -bulky methylketones is lost when a highly bulky protecting group is used, such as in the case of **13** ($\text{P} = \text{Tr}$, $\text{R} = t\text{-Bu}$), **15** ($\text{P} = \text{Tr}$, $\text{R} = \text{Me}$), and **16** ($\text{P} = \text{TPS}$, $\text{R} = \text{Me}$). These results demonstrate that the β -OP ($\text{P} = \text{Tr}$ or TPS) substituent does not provide induction.

Initially, we ascertained the volume effect in the protecting groups of β -bulky-substituted methylketones using the model system of methylketone **13** ($\text{P} = \text{Tr}$, $\text{R} = t\text{-Bu}$). Theoretical calculations were performed, and the lowest-energy transition states are shown in Scheme 22 and Table 8. We considered two conformers related to the C–Ph sigma-bond rotations (for details, see the Supporting Information, section S9).

Analysis of the relative energies of the transition states related to methylketone **13** ($\text{P} = \text{Tr}$, $\text{R} = t\text{-Bu}$) presented in Table 8 show that the competitive transition states out-1,5-anti-b-i (0.0 kcal/mol) and out-1,5-syn-b-i (0.3 and 0.2 kcal/mol for IEF-PCM and SMD solvation models, respectively) are similar in energy, which indicates poor 1,5-selectivity. In fact, selectivity for this reaction was not experimentally observed (dr = 50:50,

Table 5. Aldol Transition Structures Calculated at B3LYP and with Basis Set 6-31G(d,p), the SCRF Calculated in B3LYP/6-31+G(d,p) and IEF-PCM (UFF Radii) or SMD Solvation Model, and the Delocalization Energies and NBO Overlap Matrix (S) of the Stabilizing H-Bond

	TS	IEF-PCM E _{rel} (CH ₂ Cl ₂) (kcal/mol)	SMD E _{rel} (CH ₂ Cl ₂) (kcal/mol)	r (Å)	E _{NBO} (kcal/mol)	ΣE _{NBO} (kcal/mol)	S _{<X-HC>}	
X = Cl	in-1,5- <i>anti</i> -b	0.9	1.6	r _{O-HC} = 2.71	LP _{O1} = 0.07 LP _{O2} = 0.78	0.85	0.041 0.075	
	Cl-in-1,5- <i>anti</i>	7.6	8.1	r _{Cl-HC} = 2.59	LP _{Cl1} = 0.69 LP _{Cl2} = 0.35 LP _{Cl3} = 3.50	4.5	0.082 0.053 0.16	
	out-1,5- <i>anti</i> -a	2.0	2.0	-	-	-	-	
	in-1,5- <i>syn</i>	6.4	7.1	r _{O-HC} = 2.46	LP _{O1} = 1.42 LP _{O2} = 0.08	1.7	-0.12 0.023	
				r _{Cl-HC} = 3.34	LP _{Cl2} = 0.18		-0.045	
	Cl-in-1,5- <i>syn</i>	3.6	2.2	r _{Cl-HC} = 3.00	LP _{Cl1} = 0.09 LP _{Cl2} = 0.82 LP _{Cl3} = 0.27	1.2	-0.031 -0.081 -0.044	
					out-1,5- <i>syn</i> -a		0.0	0.0
	X = F	in-1,5- <i>anti</i> -b	0.0	0.4	r _{O-HC} = 2.48	LP _{O1} = 0.44 LP _{O2} = 1.36	1.8	-0.075 -0.11
		F-in-1,5- <i>anti</i>	6.3	6.3	r _{F-HC} = 2.20	LP _{F1} = 1.41 LP _{F2} = 0.09 LP _{F3} = 2.15	3.7	0.10 0.022 0.10
		out-1,5- <i>anti</i> -b	2.1	1.7	-	-	-	-
in-1,5- <i>syn</i>		4.7	4.8	r _{O-HC} = 2.60	LP _{O1} = 0.50 LP _{O2} = 0.28	2.7	0.075 0.044	
				r _{F-HC} = 2.37	LP _{F1} = 0.59 LP _{F2} = 1.22 LP _{F3} = 0.11		0.067 0.078 0.021	
F-in-1,5- <i>syn</i>		2.4	2.3	r _{F-HC} = 2.22	LP _{F1} = 1.63 LP _{F2} = 0.37 LP _{F3} = 1.28	3.3	0.11 0.042 0.075	
out-1,5- <i>syn</i> -a		0.3	0.0	-	-	-	-	

1,5-anti:1,5-syn), which underscores the volume effect of the β -OTr group in the erosion of the 1,5-selectivity. In addition, the volume of the β -OTr group induced strong repulsions that prevented the formation of H-bonds in the high-energy “in” conformers.

The effect of the protecting group becomes more evident by analysis of the relative energies of the “out” transition states of the β -*t*-Bu methylketones in Figure 2. The same energy profile was obtained for TMS- and Bn-protected methylketones. However, with the trityl protecting group, the energies of the **out-1,5-anti-b** and **out-1,5-syn-b** transition states were lowered.

In view of these results, the loss of 1,5-syn selectivity of methylketone **13** ($P = \text{Tr}$, $R = t\text{-Bu}$) is reasonably assumed to arise from the new repulsive interactions introduced into the system from the trityl protecting group. Analysis of the geometries presented in Scheme 22 indicates that the trityl group, which is bulkier than a *tert*-butyl group, justifies the 1 kcal/mol stability of **out-1,5-syn-b-i** over **out-1,5-syn-a-i** (Table 8). Therefore, the **out-1,5-syn-b-i** conformer keeps the β -OTr group far from the ring in the transition state but drives the β -*tert*-butyl group in the direction of the ring and the boron ligands. A similar situation occurs with the **out-1,5-anti-b-i** conformer, which keeps the β -OTr group away from the ring while directing the β -*t*-Bu group with the π -system enolate. Thus, the transition states **out-1,5-syn-b-i** and **out-1,5-anti-b-i** have lower relative energies; however, because of the unfavorable

interactions from the β -*t*-Bu group, there is no energetic discrimination between them.

The transition states related to the models of the β -alkoxy- β -methyl methylketones that involve Bn, TMS, and Tr protecting groups were also studied (see the Supporting Information, sections S10, S11, and S12, for the relative energies of all the transition states and for values of the lowest energies and geometries). The transition-state energies for these systems are represented in Figure 3.

As expected, the methylketones that contain a small β -Me substituent and a benzyl protecting group behave according to Goodman's induction model, which leads to high 1,5-*anti* selectivities because the **in-1,5-anti** is the lowest-energy conformation and because the transition state contains a stabilizing H-bond ($r_{\text{O-HC}} = 2.35$ Å and $E_{\text{HB}} = 3.0$ kcal/mol). The competitive **TS-out-1,5-syn-a** conformer was 0.8 kcal/mol more energetic than the **in-1,5-anti** conformer. Experimentally, we obtained 1,5-*anti* adducts in high selectivities ($\text{dr} > 95:05$),^{6d} which is in accordance with the theoretical results. However, β -methyl methylketones with bulky protecting groups such as TBS, Tr, and TPS led to equimolar mixtures of the 1,5-*anti* and 1,5-*syn* adducts. This scenario occurred for β -OTMS β -methyl methylketone because the lowest-energy transition-states conformers (**out-1,5-anti-b** and **out-1,5-syn-a**) showed relative energies of 0 kcal/mol. The system that contained a β -OTr protecting group exhibited similar relative energies of 0 kcal/mol

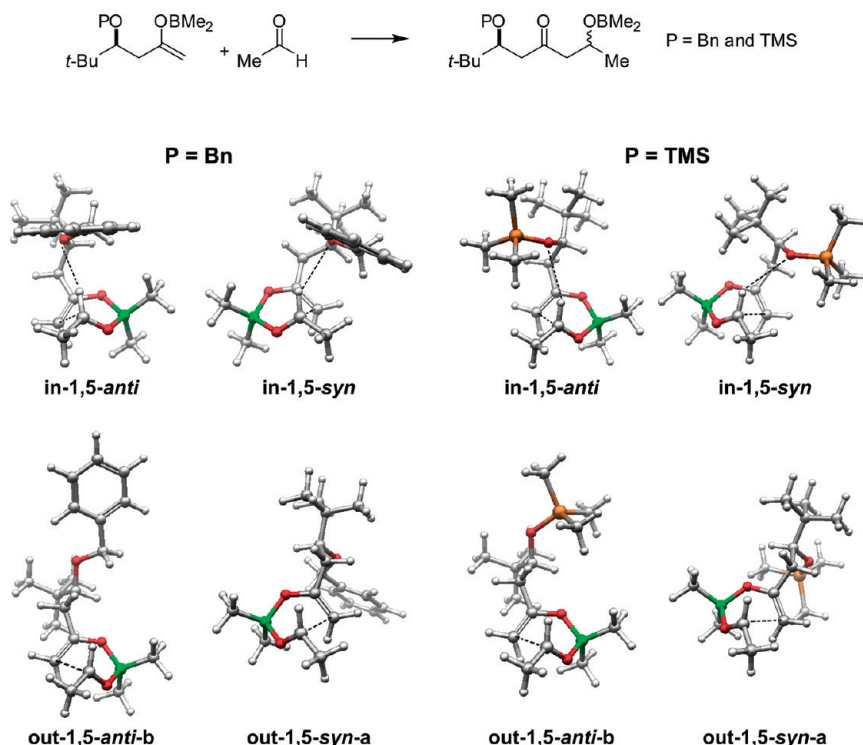
Scheme 20. Aldol Transition Structures of β -*tert*-Butyl Dimethyl Boron Enolate and Ethanal

Table 6. Aldol Transition Structures Calculated at B3LYP and with Basis Set 6-31G(d,p), the SCRf in B3LYP/6-31+G(d,p) and IEF-PCM (UFF Radii) or SMD Solvation Models, and Delocalization Energies and NBO Overlap Matrix (S) of the Stabilizing H-Bond

TS	IEF-PCM $E_{\text{rel}}(\text{Et}_2\text{O})$ (kcal/mol)	SMD $E_{\text{rel}}(\text{Et}_2\text{O})$ (kcal/mol)	r (Å)	E_{NBO} (kcal/mol)	ΣE_{NBO} (kcal/mol)	$S_{\langle X-H \rangle}$
P = Bn	in-1,5- <i>anti</i>	0.8	1.4	$r_{\text{O-HC}} = 2.71$	$\text{LP}_{\text{O1}} = 0.07$ $\text{LP}_{\text{O2}} = 0.47$	0.54 0.046 0.055
	out-1,5- <i>anti-b</i>	0.9	0.9	-	-	-
	in-1,5- <i>syn</i>	2.9	3.2	$r_{\text{O-HC}} = 2.98$	$\text{LP}_{\text{O1}} = 0.03$ $\text{LP}_{\text{O2}} = 0.16$	0.19 0.027 0.038
	out-1,5- <i>syn-a</i>	0.0	0.0	-	-	-
P = TMS	in-1,5- <i>anti</i>	4.7	4.8	$r_{\text{O-HC}} = 2.87$	$\text{LP}_{\text{O1}} = 0.08$ $\text{LP}_{\text{O2}} = 0.21$	0.29 0.039 0.051
	out-1,5- <i>anti-b</i>	1.0	0.9	-	-	-
	in-1,5- <i>syn</i>	5.0	5.5	$r_{\text{O-HC}} = 2.95$	$\text{LP}_{\text{O1}} = 0.16$	0.16 0.048
	out-1,5- <i>syn-a</i>	0.0	0.0	-	-	-

for **out-1,5-syn-b** and 0.3 kcal/mol for **out-1,5-anti-b**, which is in agreement with our experimental results.

Thus, for the methylketone **15** (P = Tr, R = Me), the **out-1,5-syn-b** and **out-1,5-anti-b** transition states represent the conformation in which the β -OTr substituent is as far as possible from the ring. No energetic discrimination between the conformations occurred because of the identical β -Me repulsive interactions with the ring; this situation is identical to that of methylketone **13** (P = Tr, R = *t*-Bu).

β -Aryl- β -Triphenylmethoxy Methylketones. The aldol reactions involving the methylketones **17** (P = Tr, R = *p*-NO₂C₆H₄) and **18** (P = TPS, R = *p*-NO₂C₆H₄) showed 1,5-*anti* induction. This result was unexpected because β -alkoxy- β -aryl methylketones lead to high 1,5-*anti* selectivities when a

benzylic protecting group is present and to poor 1,5-*syn* selectivities when bulky protective groups such as TBS and *t*-Bu^{6c,d} are used. Furthermore, β -alkyl- β -OTr methylketones did not exhibit 1,5-induction sense.

Theoretical calculations were performed to investigate the effect of β -OBn, β -OTMS, and β -OTr as protecting groups in β -aryl methylketones (sections S13, S14, and S15 in the Supporting Information contain the energies of all the transition states and the values for the lowest energies). Figure 4 shows the relative energies of the found transition states.

In the case of methylketone **33** (P = Bn, R = *p*-NO₂C₆H₄), the competitive transition states were characterized, and the **TS-in-1,5-anti** (0 kcal/mol) conformer was found to be lower in energy than the **Ts-out-1,5-syn-a** conformer by 1.0 kcal/mol.

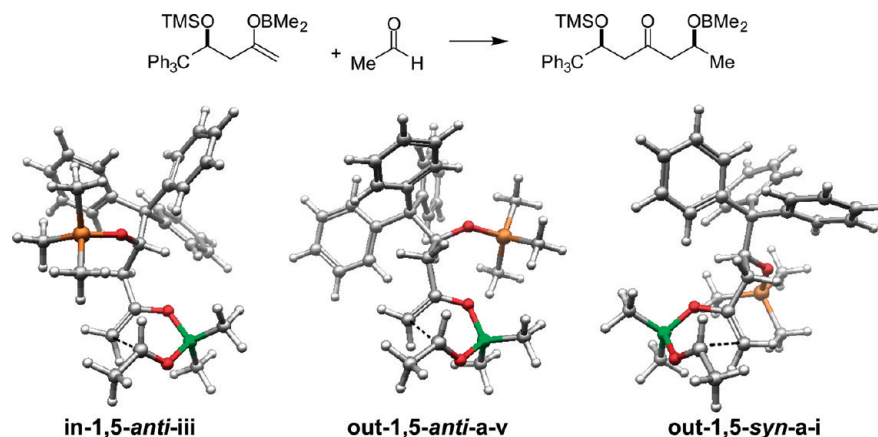
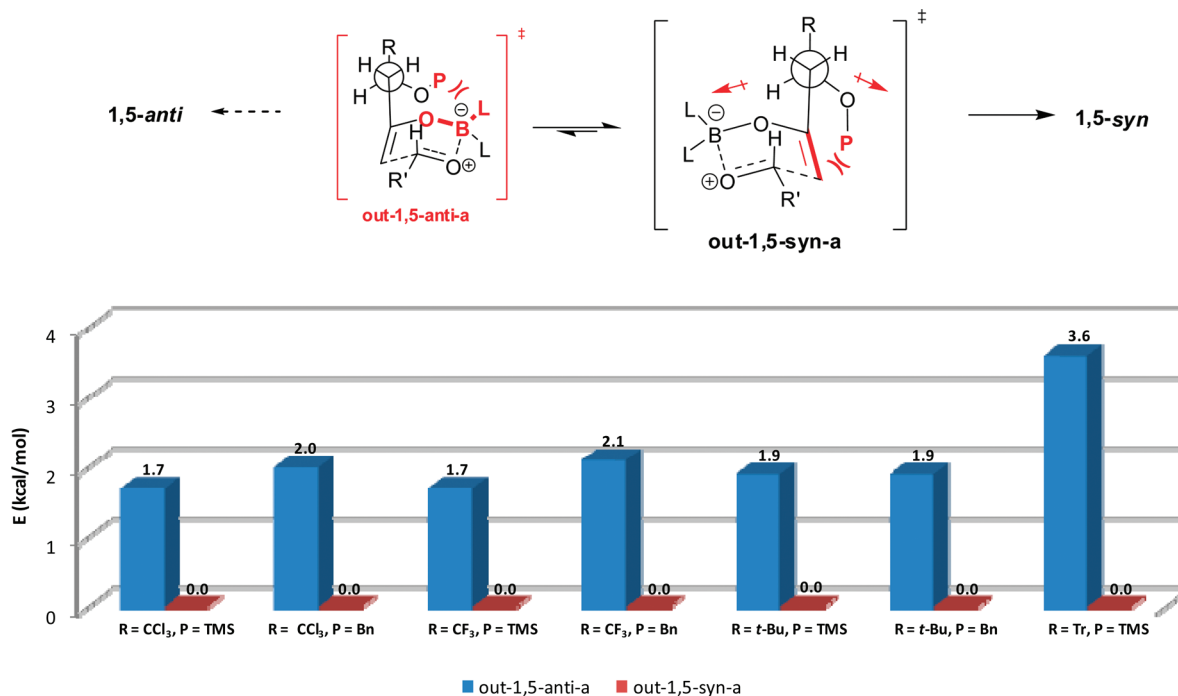
Scheme 21. Aldol Transition Structures of β -Triphenylmethyl- β -Trimethylsilyloxy Dimethyl Boron Enolate and Ethanal

Table 7. Aldol Transition Structures Calculated at B3LYP and with Basis Set 6-31G(d,p), the SCRF in B3LYP/6-31+G(d,p) and IEF-PCM (UFF Radii) or SMD Solvation Models, and the Delocalization Energies and NBO Overlap Matrix (S) of the Stabilizing H-Bond

TS	IEF-PCM $E_{\text{rel}}(\text{Et}_2\text{O})$ (kcal/mol)	SMD $E_{\text{rel}}(\text{Et}_2\text{O})$ (kcal/mol)	r (Å)	ΣE_{NBO} (kcal/mol)
in-1,5-anti-iii	6.3	6.5	$r_{\text{O-HC}} = 3.45$	0.0
out-1,5-anti-a-v	3.4	3.6	-	-
in-1,5-syn	<i>not found</i>			
out-1,5-syn-a-i	0.0	0.0	-	-

Figure 1. Energy profiles of the out-1,5-anti-a and out-1,5-syn-a transition states of β -bulky methylketones.

This large energy difference is in agreement with the experimental results ($\text{dr} > 95:05$, 1,5-*anti*:1,5-*syn*) and with the initial model of Goodman, in which the TS-in-1,5-*anti* transition state contains stabilizing H-bonds ($r_{\text{O-HC}} = 2.39$ Å and $E_{\text{HB}} = 2.8$ kcal/mol). Additionally, the TMS protecting group in the same substitution pattern (β -*p*-NO₂C₆H₄) leads to the lower-energy competitive transition states out-1,5-*anti-b* (0.4 kcal/mol)

and in-1,5-*syn* (0 kcal/mol) in an energy profile that represents a reversal in selectivity and a modest 1,5-*syn* aldol adduct preference. This result is in perfect agreement with the experimentally obtained results ($\text{dr} \sim 70:30$, 1,5-*syn*:1,5-*anti*) and also in accordance with the model proposed by Goodman.

The model used in the study of methylketone 17 (P = Tr, R = *p*-NO₂C₆H₄) led to the lowest-energy competitive

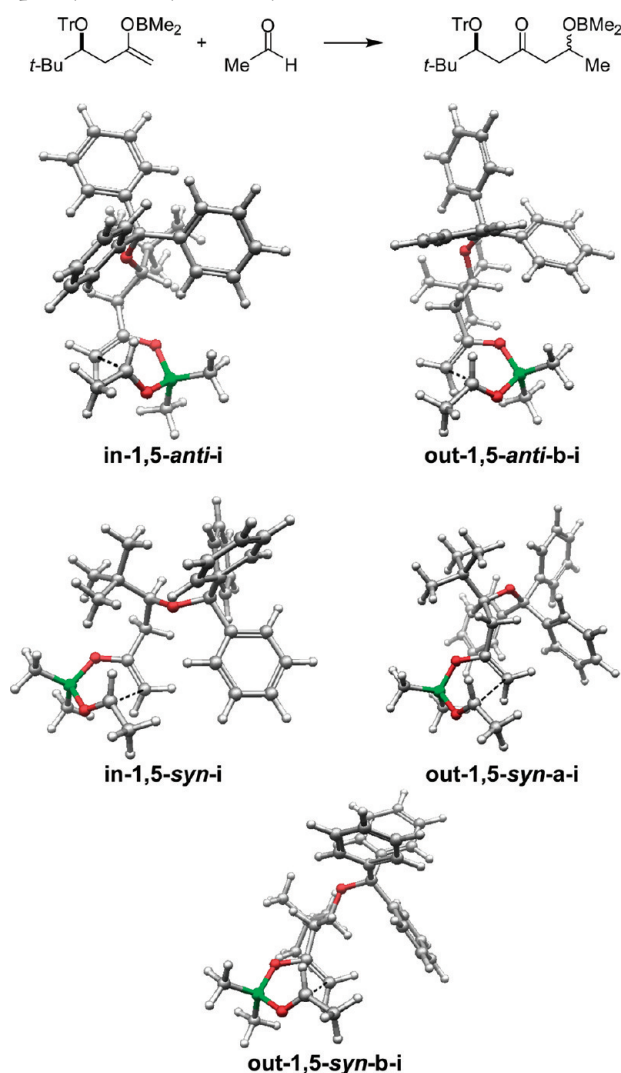
Scheme 22. Aldol Transition Structures of β -*tert*-Butyl- β -triphenylmethoxy Dimethyl Boron Enolate and Ethanal

Table 8. Aldol Transition Structures Calculated at B3LYP and with Basis Set 6-31G(d,p), the SCRF in B3LYP/6-31+G(d,p) and IEF-PCM (UFF Radii) or SMD Solvation Model, and the Delocalization Energies and NBO Overlap Matrix (S) of the Stabilizing H-Bond

TS	IEF-PCM $E_{\text{rel}}(\text{Et}_2\text{O})$ (kcal/mol)	SMD $E_{\text{rel}}(\text{Et}_2\text{O})$ (kcal/mol)	r (Å)	ΣE_{NBO} (kcal/mol)
in-1,5-anti-i	14.1	14.1	$r_{\text{O-HC}} = 3.55$	0.0
out-1,5-anti-b-i	0.0	0.0	-	-
in-1,5-syn-i	6.8	7.3	$r_{\text{O-HC}} = 3.54$	0.0
out-1,5-syn-a-i	1.2	1.4	-	-
out-1,5-syn-b-i	0.3	0.2	-	-

transition states **out-1,5-anti-b** and **out-1,5-syn-b** with energy values of 0 and 0.9 kcal/mol, respectively. These conformations keep the β -OTr substituent as far from the ring as possible, thereby reducing the system energy. However, unlike the situation with the β -alkyl substituted methylketones ($R = \text{Me}$ and $t\text{-Bu}$), here we observe a strong energy discrimination between the **out-1,5-anti-b** and **out-1,5-syn-b** conformers, with a preference for the formation of the 1,5-*anti* aldol adduct.

These results are in agreement with our experimental results ($\text{dr} \sim 80:20$, 1,5-*anti*:1,5-*syn*).

As shown in Scheme 23, in the **TS-out-1,5-syn-b-ii** transition state, the highly polarized $p\text{-NO}_2\text{C}_6\text{H}_4$ group eclipses the oxygen enolate, which leads to steric repulsions between these substituents and raises the energy of the system. However, the more energetically favorable **TS-out-1,5-anti-b-ii** keeps the β - $p\text{-NO}_2\text{C}_6\text{H}_4$ substituent in a position opposite the enolate oxygen, which minimizes the dipole moment and reduces the steric repulsions of the system. In addition, this conformer allows a π -stacking stabilization between the aromatic ring systems and the enolate.

The **out-1,5-anti-b** conformation is always lower in energy than the **out-1,5-syn-b** conformation, irrespective of the protecting group for $p\text{-NO}_2\text{C}_6\text{H}_4$ -substituted methylketones. This situation is not true for β -alkyl-substituted methylketones ($R = \text{Me}$ and $t\text{-Bu}$), which reinforces the premise of greater polarizability of the aromatic system.

CONCLUSIONS

From this systematic study involving aldol reactions of boron enolates of methylketones (with different stereoelectronic properties in the β -alkyl substituents and in the β -protecting groups) and several achiral aldehydes (aliphatic, α,β -unsaturated, and aromatic aldehydes), we conclude that the levels of selectivity observed also depend on the nature of the β -alkyl substituents and not only on the electronic nature of the β -protecting group, as previously described. These observations were corroborated by theoretical studies conducted using DFT. New studies are still required in order to investigate the generality of the 1,5-*syn* induction. We speculate that the results presented by Paterson in the synthesis of the C27–C51 fragment of spongistatin 1^{3f} (Scheme 3) are included in the induction model proposed in this paper. The highly substituted F-subunit should provide the required β -substituent volume that direct the stereochemical bias to 1,5-*syn* selectivity. New efforts are underway in the direction of a full comprehension of the factors that govern the 1,5-*syn* selectivity and the development of a 1,5-*syn* aldol methodology with synthetic utility.

EXPERIMENTAL SECTION

Materials and Methods. Unless noted, all reactions were performed under an atmosphere of argon in flame-dried glassware with magnetic stirring. Dichloromethane, triethylamine (Et_3N), 2,6-lutidine, and dimethylformamide (DMF) were distilled from CaH_2 . Dimethyl sulfoxide (DMSO) was distilled under reduced pressure from CaH_2 and stored over molecular sieves. THF and diethyl ether were distilled from sodium/benzophenone. Oxalyl chloride was distilled immediately prior to use. The purification of reaction products was performed by flash column chromatography using silica gel (230–400 mesh). Analytical thin-layer chromatography was performed on silica-gel 60 and GF (5–40- μm thickness) plates. Visualization was accomplished with UV light and phosphomolybdic acid followed by heating. Optical rotations were measured with a sodium lamp and are reported as follows: $[\alpha]_D^{25}$ (c g/100 mL, solvent). Melting points are uncorrected. For the Infrared spectra, wavelengths of maximum absorbance (max) are quoted in wavenumbers (cm^{-1}). ^1H and proton-decoupled ^{13}C NMR spectra were taken in C_6D_6 , CDCl_3 or CD_3OD at 250 MHz (^1H) and 62.5 MHz (^{13}C), 400 MHz (^1H) and 100 MHz (^{13}C) or at 500 MHz (^1H) and 125 MHz (^{13}C). The chemical shifts (δ) are reported in ppm using solvent as an internal standard (C_6D_6 at 7.16 ppm, CDCl_3 at 7.26 ppm, and CD_3OD at 3.30 ppm for ^1H NMR spectra and C_6D_6 at 128.0 ppm, CDCl_3 at 77.0 ppm, and CD_3OD at 49.0 ppm for ^{13}C NMR spectra). Data are reported as follows: s = singlet, d = doublet, t = triplet, q = quartet, quint =

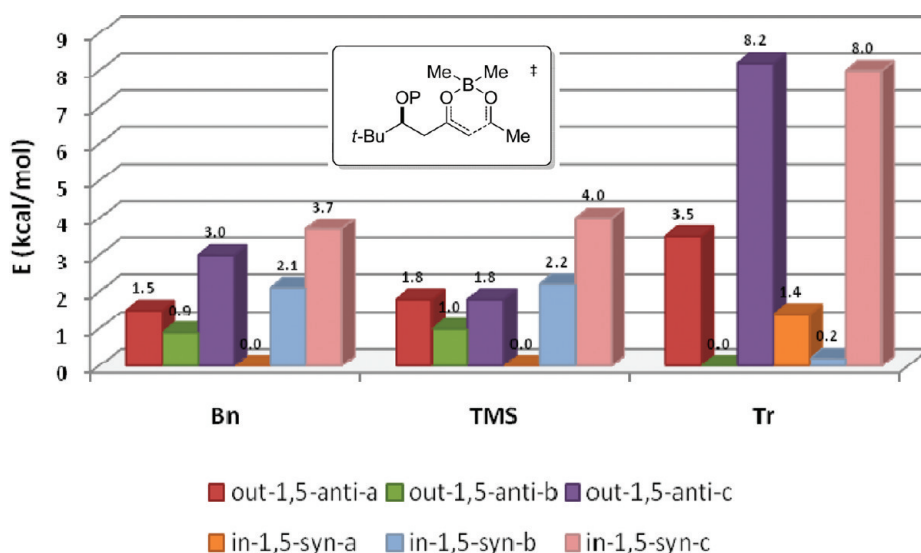


Figure 2. Relative transition-state energies (IEF-PCM) of β -*t*-Bu-substituted methylketones.

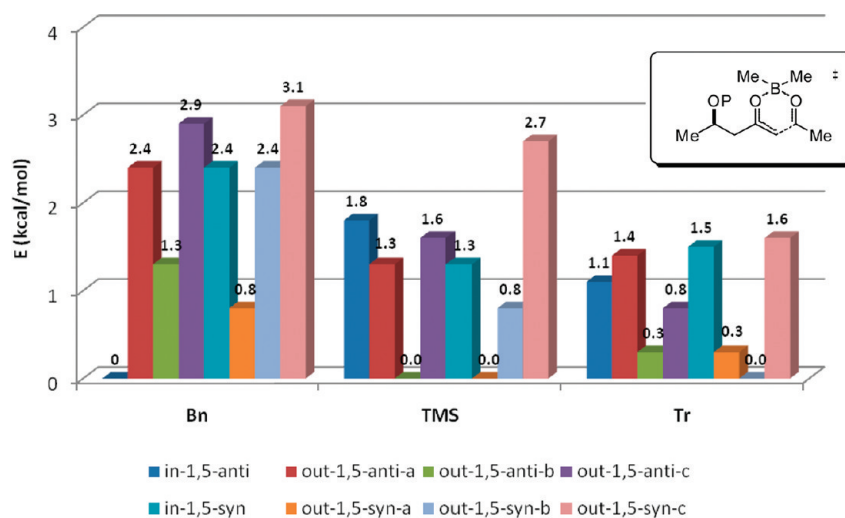


Figure 3. Relative transition-state energies (IEF-PCM) of β -Me-substituted methylketones.

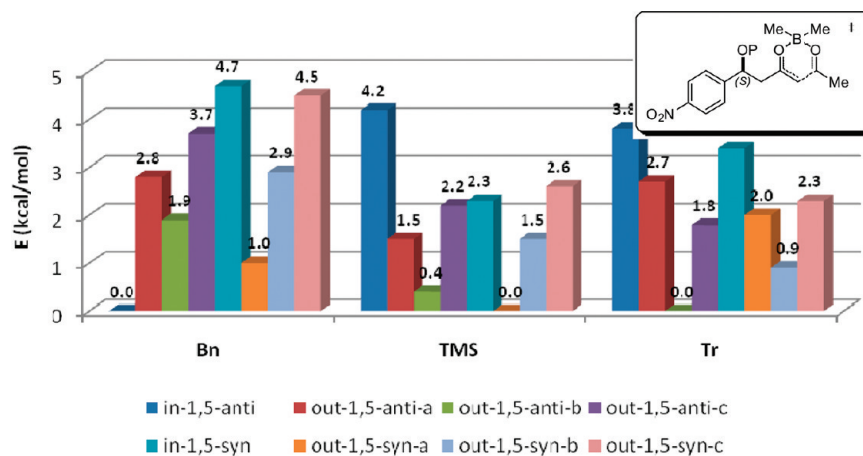
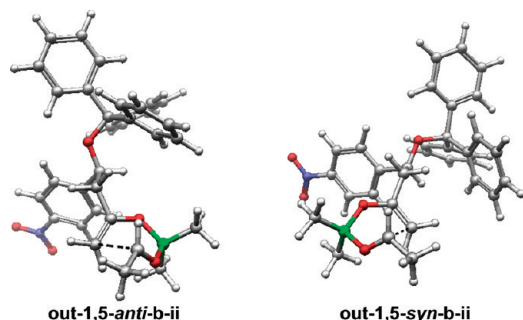


Figure 4. Relative transition-state energies (IEF-PCM) of β -*p*-NO₂C₆H₄-substituted methylketones.

quintuplet, sext = sextet, br s = broad singlet, dd = doublet of doublets, dt = doublet of triplets, ddd = doublet of doublet of doublets, tt = triplet of triplets, m = multiplet; coupling constant(s) in Hz; integration. The signals of the minor isomers are stated in brackets. High-resolution

mass spectrometry (HRMS) were measured using electrospray ionization (ESI) or using electron ionization (EI). The parent ions ($[M + H]^+$, $[M + Na]^+$, $[M - CH_3]^+$, $[M - C_4H_9]^+$, $[M - C_6H_5]^+$) are quoted. The preparation of methylketones 11, 12, 13, 15, 17 and the

Scheme 23



aldol adducts 24a–g, 25a–g, 26a–h, 27a–h, 47a–e, 48a–e, 49a–e, 50a–e, 51a–f, 52a–f is described in ref 9.

Preparation of Methylketones. (+)-(*R*)-5,5-Dimethyl-4-(triphenylsilyloxy)hexan-2-one (**14**). A solution of alcohol **20** (200 mg, 1.39 mmol), AgOTf (426 mg, 3.53 mmol), and 2,6-lutidine (0.24 mL, 2.02 mmol) in anhydrous CH_2Cl_2 (10 mL) was cooled to 0 °C. TPSCI (1.04 g, 3.53 mmol) was added, and the resulting suspension was stirred for 5 min at 0 °C and 1 h at room temperature. After this period, the crude reaction was filtered through a pad of Celite. The filtrate was washed with saturated aqueous NaHCO_3 (2 \times 50 mL) and then with brine (2 \times 50 mL). The organic phase was subsequently dried over MgSO_4 and concentrated. The residue was purified by flash column chromatography (silica gel 200–400 mesh) using a mixture of hexane/ethyl acetate (90:10) as eluent, which provided 461 mg (82%) of **14** as a white solid. $[\alpha]_D^{20}$ +4.0 (*c* 1.31; CHCl_3). R_f 0.53 (10% EtOAc in hexane). Mp 73–76 °C. IR (neat) 3070, 3051, 2962, 2908, 2870, 1717, 1711, 1589, 1479, 1468, 1429, 1394, 1366, 1292, 1265, 1161, 1117, 1086, 1074, 1022, 997, 878, 739, 710, 700 cm^{-1} . ^1H NMR (250 MHz; C_6D_6) δ 0.85 (s, 9H); 1.40 (s, 3H); 2.21 (dd, J = 3.0 and 17.8 Hz, 1H); 2.53 (dd, J = 7.1 and 17.8 Hz, 1H); 4.49 (dd, J = 3.0 and 7.1 Hz, 1H); 7.16–7.23 (m, 9H); 7.84–7.90 (m, 6H). ^{13}C NMR (62.5 MHz; C_6D_6) δ 26.1; 29.8; 35.6; 47.3; 76.2; 128.0; 130.0; 135.6; 136.2; 204.9. HRMS (ESI TOF-MS): calcd for $\text{C}_{26}\text{H}_{31}\text{O}_2\text{Si}$ 403.2093; found 403.2056.

(*RS*)-4-(Triphenylsilyloxy)pentan-2-one (**16**). A solution of alcohol **37** (730 mg, 7.0 mmol), AgOTf (1.80 g, 7.0 mmol), and 2,6-lutidine (1.0 mL, 8.6 mmol) in anhydrous CH_2Cl_2 (12 mL) was cooled to 0 °C. TPSCI (2.06 g, 7.0 mmol) was added, and the resulting suspension was stirred for 5 min at 0 °C and 1 h at room temperature. After this period, the crude reaction was filtered through a pad of Celite, and the filtrate was washed with saturated aqueous NaHCO_3 (2 \times 50 mL) and then with brine (2 \times 50 mL). The organic phase was subsequently dried over MgSO_4 and concentrated. The residue was purified by flash column chromatography (silica gel 200–400 mesh) using a mixture of hexane/ethyl acetate (80:20) as eluent, which provided the compound **39** as an oil.

DMSO (1.19 mL, 16.8 mmol) was added dropwise to a stirred solution of oxalyl chloride (0.76 mL, 8.61 mmol) in CH_2Cl_2 (43 mL) at –78 °C, and the mixture was stirred for 30 min. A solution of the alcohol **39** (2.54 g, 7.0 mmol) in CH_2Cl_2 (18 mL) was added dropwise via cannula, and the mixture was stirred at –78 °C for 30 min. Et_3N (4.9 mL, 35.0 mmol) was added dropwise. The suspension was allowed to slowly warm to room temperature and was stirred for 1 h. The reaction was quenched with the addition of a saturated aqueous NH_4Cl solution (20 mL). The phases were separated, and the aqueous phase was extracted with EtOAc (3 \times 50 mL). The organic phase was washed with water (2 \times 25 mL) and brine (2 \times 25 mL), dried over MgSO_4 , filtered, and concentrated under reduced pressure. The residue was purified by flash column chromatography (silica gel 200–400 mesh) using a mixture of hexane/ethyl acetate (80:20) as eluent, which provided 1.51 g (60%, two steps) of **16** as a white solid. R_f 0.54 (20% EtOAc in hexane). Mp 55–58 °C. IR (neat) 3070, 3051, 2972, 2930, 1715, 1589, 1485, 1429, 1375, 1337, 1265, 1117, 1086, 1020, 901, 739, 712, 702 cm^{-1} . ^1H NMR (250 MHz; C_6D_6) δ 1.14 (d, J = 6.1 Hz, 3H); 1.62 (s, 3H); 2.13 (dd, J = 6.1 and 15.6 Hz, 1H); 2.49

(dd, J = 6.1 and 15.6 Hz, 1H); 4.54 (sext, J = 6.1 Hz, 1H); 7.16–7.23 (m, 9H); 7.14–7.79 (m, 6H). ^{13}C NMR (125 MHz; C_6D_6) δ 24.0; 30.3; 52.9; 66.8; 128.2; 130.3; 135.1; 135.9; 205.0. HRMS (EI TOF-MS): calcd for $\text{C}_{17}\text{H}_{19}\text{O}_2\text{Si}$ [M – C_6H_5] $^+$ 283.1154; found 283.1162.

(*RS*)-4-(4-Nitrophenyl)-4-(triphenylsilyloxy)butan-2-one (**18**). To a solution of alcohol **40** (1.01 g, 4.78 mmol) in DMF (15 mL) under argon atmosphere was added pyridine (3.85 mL; 47.8 mmol) followed by AgNO_3 (3.25 g; 19.1 mmol), and the mixture was stirred until the solid was completely dissolved. Then, TPSCI (5.63 g; 19.1 mmol) was added in one portion, and the resulting suspension was stirred for 18 h at room temperature. After this period, the crude reaction was filtered, and the white solid was washed with Et_2O . The organic phase was washed with water (2 \times 25 mL) and brine (2 \times 25 mL), dried over MgSO_4 , filtered, and concentrated under reduced pressure. The residue was purified by flash column chromatography (silica gel 200–400 mesh) using a mixture of hexane/dichloromethane/ethyl acetate (50:40:10) as the eluent, which provided 1.63 g (73%) of **18** as a pale yellow solid. R_f 0.80 (hexane/ CH_2Cl_2 /EtOAc, 50:10:40). ^1H NMR (250 MHz; C_6D_6) δ 1.61 (s, 3H); 2.28 (dd, J = 5.5 and 16.3 Hz, 1H); 2.75 (dd, J = 7.0 and 16.4 Hz, 1H); 5.53 (t, J = 5.5 Hz, 1H); 7.01 (d, J = 8.7 Hz, 2H); 7.22 (m, 9H); 7.71 (m, 6H); 7.80 (d, J = 8.7 Hz, 2H). ^{13}C NMR (62.5 MHz; C_6D_6) δ 30.4; 53.2; 71.6; 123.4; 127.1; 128.2; 130.5; 134.0; 135.8; 147.5; 150.6; 203.7. HRMS (ESI TOF-MS): calcd for $\text{C}_{28}\text{H}_{26}\text{NO}_4\text{Si}$ 468.1631; found 468.1647.

(*RS*)-3-Hydroxy-*N*-methoxy-*N*-methyl-4,4,4-triphenylbutanamide (**65**). Lithium diisopropylamide (LDA) was generated by the addition of *n*-butyllithium (4.7 mL, 7.33 mmol, 1.6 M solution in hexanes) to a solution of diisopropylamine (1.00 mL, 7.3 mmol) in THF (5.0 mL) at –78 °C. After 10 min, a solution of Weinreb amide **64** (0.8 mL, 7.3 mmol) in THF (2.5 mL) was added via cannula, and the resulting solution was stirred at –78 °C for 30 min. A solution of aldehyde **63** (1.0 g, 3.65 mmol) in THF (5.0 mL) was added via cannula, and the solution was stirred at –78 °C for 40 min. The reaction was quenched at –78 °C by the addition of saturated aqueous NH_4Cl (10 mL), and the mixture was warmed to room temperature. The mixture was diluted with EtOAc. The aqueous washings were extracted with EtOAc (3 \times 50 mL). The combined organic layers were washed with saturated aqueous NaHCO_3 (2 \times 50 mL) and brine (2 \times 50 mL), dried over MgSO_4 , filtered, and concentrated under reduced pressure, which provided 1.37 g (99%) of **65** as a white solid. R_f 0.30 (30% EtOAc in hexane). Mp 117–120 °C. IR (neat) 3450, 3088, 3057, 3034, 3020, 2970, 2937, 1645, 1597, 1495, 1447, 1423, 1389, 1267, 1180, 1107, 1088, 1036, 1001, 991, 895, 737, 706, 652, 640 cm^{-1} . ^1H NMR (400 MHz; CDCl_3) δ 2.06 (dd, J = 10.7 and 16.1 Hz, 1H), 2.77 (d, J = 16.1 Hz, 1H), 3.04 (d, J = 3.7 Hz, 1H), 3.15 (s, 3H), 3.43 (s, 3H), 5.84 (dd, J = 3.7 and 9.5 Hz, 1H), 7.18 (t, J = 7.4 Hz, 3H), 7.27 (t, J = 7.4 Hz, 6H), 7.39 (d, J = 7.4 Hz, 6H). ^{13}C NMR (62.5 MHz; CDCl_3) δ 32.0; 36.0; 61.0; 61.3; 70.2; 126.2; 127.7; 129.9; 144.5; 173.5. HRMS (ESI TOF-MS): calcd for $\text{C}_{24}\text{H}_{26}\text{NO}_3$ 376.1913; found 376.1879.

(*RS*)-3-(*tert*-Butyldimethylsilyloxy)-*N*-methoxy-*N*-methyl-4,4,4-triphenylbutanamide (**66**). TBSOTf (0.7 mL, 3.1 mmol) was added dropwise to a solution of alcohol **65** (1.0 g, 2.7 mmol) and 2,6-lutidine (0.5 mL, 3.9 mmol) in CH_2Cl_2 (5.0 mL). After 1 h, the reaction was quenched by the addition of water (10 mL). The phases were separated, and the aqueous phase was extracted with EtOAc (3 \times 50 mL). The organic phase was washed with water (2 \times 25 mL) and brine (2 \times 25 mL), dried over MgSO_4 , filtered, and concentrated under reduced pressure. The residue was purified by flash column chromatography (silica gel 200–400 mesh) using a mixture of hexane/ethyl acetate (80:20) as the eluent, which provided 1.13 g (85%) of **66** as a white solid. R_f 0.48 (30% EtOAc in hexane). Mp 179–181 °C. IR (neat) 3055, 2957, 2930, 2856, 1659, 1597, 1495, 1472, 1447, 1421, 1389, 1265, 1180, 1101, 993, 959, 897, 831, 777, 739, 706 cm^{-1} . ^1H NMR (400 MHz; CDCl_3) δ –0.07 (s, 3H), –0.04 (s, 3H), 0.59 (s, 9H), 1.94 (dd, J = 5.3 and 17.2 Hz, 1H), 2.58 (d, J = 17.2 Hz, 1H), 3.15 (s, 3H), 3.35 (s, 3H), 6.12 (d, J = 7.8 Hz, 1H), 7.11 (br s, 3H), 7.23 (br s, 6H), 7.39 (br s, 6H). ^{13}C NMR (62.5 MHz; CDCl_3) δ –5.6; –4.4; 18.1; 25.5; 32.3; 39.3; 60.8; 62.2; 71.3; 125.7; 127.9;

129.1; 146.6; 172.9. HRMS (ESI TOF-MS): calcd for $C_{30}H_{40}NO_3Si$ 490.2777; found 490.2766.

(RS)-4-(tert-Butyldimethylsilyloxy)-5,5,5-triphenylpentan-2-one (19). To a solution of Weinreb amide **66** (50 mg, 0.10 mmol) in THF (1.8 mL) was added MeLi (0.71 mL, 0.50 mmol, 0.70 M in Et₂O) dropwise at $-78^{\circ}C$. The reaction mixture was stirred for 40 min. The reaction was quenched at $-78^{\circ}C$ by the addition of saturated aqueous NH_4Cl (5 mL), and the mixture was warmed to room temperature. The mixture was diluted with EtOAc. The aqueous washings were extracted with EtOAc (3 \times 5 mL). The combined organic layers were washed with brine (2 \times 10 mL), dried over $MgSO_4$, filtered, and concentrated under reduced pressure. The residue was purified by flash column chromatography (silica gel 200–400 mesh) using a mixture of hexane/ethyl acetate (80:20) as the eluent, which provided 46 mg (99%) of **19** as a yellow solid. R_f 0.79 (20% EtOAc in hexane). Mp $171-174^{\circ}C$. IR (neat) 3057, 2955, 2928, 2854, 1715, 1495, 1447, 1360, 1265, 1103, 1005, 835, 739, 704 cm^{-1} . 1H NMR (250 MHz; $CDCl_3$) δ -0.08 (s, 3H), -0.07 (s, 3H), 0.59 (s, 9H), 1.98 (dd, J = 6.5 and 19.1 Hz, 1H), 2.03 (s, 3H), 2.72 (d, J = 19.1 Hz, 1H), 6.10 (d, J = 6.5 Hz, 1H), 7.00–7.47 (m, 15H). ^{13}C NMR (62.5 MHz; $CDCl_3$) δ -5.7; -4.4; 18.0; 25.6; 30.8; 51.3; 61.9; 70.1; 125.9; 127.7; 129.0; 146.6; 206.9. HRMS (EI TOF-MS): calcd for $C_{25}H_{27}O_2Si$ [M - C_4H_9]⁺ 387.1780; found 387.1762.

General Procedure for Methylketone Aldol Reactions. To a solution of the methylketone (1.0 equiv, 0.21 mmol) in Et₂O (5.5 mL) at $-30^{\circ}C$ was carefully added (*c*-Hex)₂BCl (2.0 equiv, 0.42 mmol), followed by the addition of Et₃N (2.1 equiv, 0.44 mmol). After the addition of Et₃N was complete (the formation of a white cloud was observed at this point), the reaction medium was immediately cooled to $-78^{\circ}C$. The corresponding aldehyde (4.0 equiv, 0.84 mmol) was added dropwise to this slurry, and the resulting mixture was stirred for 1 h. The reaction was quenched by the addition of MeOH (4.0 mL), and the resulting solution was stirred at room temperature for 30 min. The solvent was removed under reduced pressure, and the residue was purified by flash column chromatography (silica gel 200–400 mesh), which provided the aldol adducts.

(3R,7S)-7-Hydroxy-2,2,8-trimethyl-3-(triphenylsilyloxy)nonan-5-one (53a) and (3R,7R)-7-Hydroxy-2,2,8-trimethyl-3-(triphenylsilyloxy)nonan-5-one (54a). The mixture of aldol adducts **53a** and **54a** (88%, 85 mg, 0.18 mmol) was obtained as a yellow oil (65:35 diastereoselectivity) after purification by flash column chromatography (silica gel 200–400 mesh) using a mixture of hexane/ethyl acetate (80:20) as the eluent. R_f 0.56 (20% EtOAc in hexane). IR (neat) 3580, 3070, 3053, 2962, 2908, 2874, 1709, 1589, 1479, 1470, 1429, 1394, 1366, 1265, 1115, 1088, 1063, 1028, 999, 897, 748, 710 cm^{-1} . 1H NMR (250 MHz; C_6D_6) δ 0.81–0.91 (m, 15H); 1.33–1.51 (m, 1H); 1.76 (dd, J = 1.4 and 17.6 Hz, 1H); 1.81–1.97 (m, 1H); 2.06 (dd, J = 10.1 and 17.6 Hz, 1H); (2.22 (dd, J = 2.0 and 18.0 Hz, 1H)); 2.34 (dd, J = 2.6 and 18.1 Hz, 1H); 2.41 (br s, 1H); 2.52–2.63 (m, 1H); (3.29 (dd, J = 4.1 and 9.2 Hz, 1H)); 3.56 (m, 1H); 4.41 (dd, J = 2.8 and 7.1 Hz, 1H); (4.48 (dd, J = 2.3 and 7.8 Hz, 1H)); 7.18–7.23 (m, 9H); 7.83–7.88 (m, 6H). ^{13}C NMR (62.5 MHz; C_6D_6) δ 17.5; (17.6); 18.7; (18.8); (26.2); 26.2; (33.2); 33.2; (35.5); 35.7; 46.8; (47.3); 47.4; (71.2); 71.6; (75.7); 75.8; (128.0); 128.1; (130.0); 130.1; 135.6; (135.6); 136.1; 209.6; (209.6). HRMS (ESI TOF-MS): calcd for $C_{30}H_{39}O_3Si$ 475.2668; found 475.2666.

(3S,7R)-3-Hydroxy-2,2,8,8-tetramethyl-7-(triphenylsilyloxy)nonan-5-one (53c) and (3R,7R)-3-Hydroxy-2,2,8,8-tetramethyl-7-(triphenylsilyloxy)nonan-5-one (54c). The mixture of aldol adducts **53c** and **54c** (86%, 87 mg, 0.18 mmol) was obtained as a yellow oil (63:37 diastereoselectivity) after purification by flash column chromatography (silica gel 200–400 mesh) using a mixture of hexane/ethyl acetate (80:20) as eluent. R_f 0.68 (20% EtOAc in hexane) IR (neat) 3543, 3070, 3053, 2962, 2907, 2872, 1963, 1904, 1828, 1778, 1709, 1653, 1589, 1479, 1468, 1429, 1394, 1366, 1308, 1265, 1186, 1115, 1084, 1028, 999, 943, 937, 897, 741, 710 cm^{-1} . 1H NMR (400 MHz; C_6D_6) δ 0.85 (s, 9H); (0.85 (s, 9H)); 0.86 (s, 9H); (0.87 (s, 9H)); 1.88 (dd, J = 10.4 and 17.2 Hz, 1H); (1.88 (dd, J = 1.5 and 17.2 Hz, 1H)); 2.04–2.11 (m, 1H); (2.26 (dd, J = 2.2 and 18.2 Hz, 1H)); 2.36 (dd, J = 2.6 and 18.3 Hz, 1H); 2.52 (br s, 1H); (2.59 (dd, J = 7.5

and 18.1 Hz, 1H)); 2.60 (dd, J = 7.3 and 18.1 Hz, 1H); (2.70 (br s, 1H)); (3.26 (d, J = 10.3 Hz, 1H)); 3.48 (d, J = 10.3 Hz, 1H); 4.42 (dd, J = 2.5 and 7.5 Hz, 1H); (4.48 (dd, J = 2.3 and 7.5 Hz, 1H)); 7.19–7.25 (m, 9H); 7.84–7.87 (m, 6H). ^{13}C NMR (62.5 MHz; C_6D_6) δ 25.8; (25.9); (26.2); 26.2; (34.1); 34.2; (35.5); 35.7; 44.7; (44.8); 47.5; (47.7); (74.1); 74.5; (75.6); 75.8; 128.1; (128.5); (130.0); 130.1; 135.6; (135.7); 136.1; (209.7); 210.0. HRMS (ESI TOF-MS): calcd for $C_{31}H_{40}O_3SiNa$ 511.2644; found 511.2639.

(1S,5R)-1-Hydroxy-6,6-dimethyl-1-phenyl-5-(triphenylsilyloxy)heptan-3-one (53e) and (1R,5R)-1-Hydroxy-6,6-dimethyl-1-phenyl-5-(triphenylsilyloxy)heptan-3-one (54e). The mixture of aldol adducts **53e** and **54e** (68%, 72 mg, 0.14 mmol) was obtained as a yellow oil (70:30 diastereoselectivity) after purification by flash column chromatography (silica gel 200–400 mesh) using a mixture of hexane/ethyl acetate (80:20) as the eluent. R_f 0.50 (20% EtOAc in hexane). IR (neat) 3568, 3051, 2962, 2907, 2872, 1707, 1589, 1479, 1454, 1429, 1394, 1364, 1265, 1194, 1115, 1088, 1028, 932, 739, 702 cm^{-1} . 1H NMR (500 MHz; C_6D_6) δ 0.83 (s, 9H); (0.83 (s, 9H)); (1.99 (dd, J = 2.3 and 17.5 Hz, 1H)); 2.12–2.19 (m, 2H); (2.22 (dd, J = 2.3 and 18.0 Hz, 1H)); 2.25 (dd, J = 2.9 and 18.2 Hz, 1H); (2.30 (dd, J = 7.5 and 17.5 Hz, 1H)); 2.54 (dd, J = 7.7 and 18.2 Hz, 1H); (2.54 (dd, J = 7.7 and 18.0 Hz, 1H)); 2.68 (br s, 1H); (3.01 (br s, 1H)); 4.41 (dd, J = 2.9 and 7.6 Hz, 1H); (4.49 (dd, J = 2.3 and 7.8 Hz, 1H)); (4.65 (dd, J = 2.0 and 10.1 Hz, 1H)); 4.82 (dd, J = 4.7 and 7.7 Hz, 1H); 7.09–7.30 (m, 14H); 7.85–7.89 (m, 6H). ^{13}C NMR (62.5 MHz; C_6D_6) δ (26.1); 26.1; (35.5); 35.6; 47.3; (47.4); 52.1; (52.1); (69.2); 69.7; (75.6); 75.7; (125.9); 126.1; (127.4); 127.5; (128.1); 128.1; 128.4; (128.5); (130.1); 130.1; 135.6; (135.6); 136.1; 143.9; 208.5; (208.7). HRMS (ESI TOF-MS): calcd for $C_{33}H_{37}O_3Si$ 509.2512; found 509.2532.

(2RS,6RS)-6-Hydroxy-7-methyl-2-(triphenylsilyloxy)octan-4-one (55a) and (2RS,6SR)-6-Hydroxy-7-methyl-2-(triphenylsilyloxy)octan-4-one (56a). The mixture of aldol adducts **55a** and **56a** (90%, 84 mg, 0.19 mmol) was obtained as a yellow oil (50:50 diastereoselectivity) after purification by flash column chromatography (silica gel 200–400 mesh) using a mixture of hexane/ethyl acetate (80:20) as the eluent. R_f 0.44 (20% EtOAc in hexane). IR (neat) 3545, 3070, 3053, 2966, 2930, 1963, 1894, 1828, 1778, 1589, 1466, 1429, 1379, 1265, 1117, 1080, 997, 895, 748, 719 cm^{-1} . 1H NMR (400 MHz; C_6D_6) δ (0.80 (d, J = 6.8 Hz, 3H)); 0.81 (d, J = 6.8 Hz, 3H); 0.87 (d, J = 6.8 Hz, 3H); 1.11–1.13 (m, 3H); 1.43–1.51 (m, 1H); 2.04–2.22 (m, 3H); 2.47–2.52 (m, 1H); 2.83 (br s, 1H); 3.64–3.69 (m, 1H); 4.49–4.60 (m, 1H); 7.20–7.21 (m, 9H); 7.75–7.77 (m, 6H). ^{13}C NMR (62.5 MHz; C_6D_6) δ 17.6; (17.6); 18.7; (18.7); 24.0; (33.3); 33.3; (47.3); 47.6; 52.9; (53.0); (66.7); 66.7; 71.8; (71.9); 128.2; (130.3); 130.3; (135.0); 135.1; 135.9; (209.7); 209.8. HRMS (ESI TOF-MS): calcd for $C_{27}H_{33}O_3Si$ 433.2199; found 433.2199.

(2RS,6RS)-6-Hydroxy-7-methyl-2-(triphenylsilyloxy)oct-7-en-4-one (55d) and (2RS,6SR)-6-Hydroxy-7-methyl-2-(triphenylsilyloxy)oct-7-en-4-one (56d). The mixture of aldol adducts **55d** and **56d** (83%, 84 mg, 0.20 mmol) was obtained as a white oil (50:50 diastereoselectivity) after purification by flash column chromatography (silica gel 200–400 mesh) using a mixture of hexane/ethyl acetate (80:20) as the eluent. R_f 0.45 (20% EtOAc in hexane). IR (neat) 3481, 3070, 3051, 2974, 2930, 1963, 1894, 1826, 1707, 1653, 1589, 1485, 1429, 1377, 1265, 1186, 1117, 1090, 1020, 995, 905, 744, 702 cm^{-1} . 1H NMR (400 MHz; C_6D_6) δ (1.12 (d, J = 6.3 Hz, 3H)); 1.12 (d, J = 6.3 Hz, 3H); 1.57 (s, 3H); 2.12–2.23 (m, 2H); 2.27–2.38 (m, 1H); 2.48–2.54 (m, 1H); 2.88 (br s, 1H); 4.35–4.41 (m, 1H); 4.48–4.60 (m, 1H); 4.77 (s, 1H); 5.00–5.01 (m, 1H); 7.20–7.22 (m, 9H); 7.74–7.77 (m, 6H). ^{13}C NMR (62.5 MHz; C_6D_6) δ (18.3); 18.4; 23.9; (48.7); 49.1; (52.9); 53.0; 66.6; (66.7); (71.0); 71.1; 110.7; (110.7); 128.2; 130.3; (130.3); (135.0); 135.1; 135.9; 146.5; (146.5); 208.7; (208.7). HRMS (ESI TOF-MS): calcd for $C_{27}H_{31}O_3Si$ 431.2043; found 431.2047.

(1RS,5RS)-1-Hydroxy-1-phenyl-5-(triphenylsilyloxy)hexan-3-one (55e) and (1SR,5RS)-1-Hydroxy-1-phenyl-5-(triphenylsilyloxy)hexan-3-one (56e). The mixture of aldol adducts **55e** and **56e** (71%, 70 mg, 0.15 mmol) was obtained as a colorless oil (50:50 diastereoselectivity) after purification by flash column chromatography (silica gel 200–400 mesh) using a mixture of hexane/ethyl acetate (80:20) as the eluent. R_f 0.38 (20% EtOAc in hexane). IR (neat) 3522,

3069, 3053, 2974, 2930, 2899, 1963, 1894, 1828, 1778, 1707, 1589, 1495, 1454, 1429, 1379, 1265, 1186, 1117, 1090, 1067, 1030, 916, 895, 739, 702 cm⁻¹. ¹H NMR (400 MHz; C₆D₆) δ 1.09 (d, *J* = 6.0 Hz, 3H); 2.02–2.10 (m, 1H); 2.26–2.37 (m, 1H); 2.39–2.52 (m, 2H); (3.13 (br s, 1H)); 3.22 (br s, 1H); 4.44–4.57 (m, 1H); 4.97–5.03 (m, 1H); 7.07–7.11 (m, 1H); 7.15–7.26 (m, 13H); 7.74–7.77 (m, 6H). ¹³C NMR (62.5 MHz; C₆D₆) δ 23.9; 52.3; (52.6); (52.8); 52.9; 66.6; (66.7); (69.7); 69.8; (126.0); 126.0; 127.4; 128.2; 128.5; (130.3); 130.3; (135.0); 135.0; 135.9; 143.9; 208.7; (208.8). HRMS (ESI TOF-MS): calcd for C₃₀H₃₀O₃SiNa 489.1862; found 489.1842.

(1*SR*,5*SR*)-5-Hydroxy-6-methyl-1-(4-nitrophenyl)-1-(triphenylsilyloxy)heptan-3-one (**57a**) and (1*SR*,5*RS*)-5-Hydroxy-6-methyl-1-(4-nitrophenyl)-1-(triphenylsilyloxy)heptan-3-one (**58a**). The mixture of aldol adducts **57a** and **58a** (69%, 0.112 g, 0.18 mmol) was obtained as a pale yellow oil (61:39 diastereoselectivity) after purification by flash column chromatography (silica gel 200–400 mesh) using a mixture of hexane/dichloromethane/ethyl acetate (50:40:10) as the eluent. *R*_f 0.50 (hexane/CH₂Cl₂/EtOAc 5:4:1). ¹H NMR (250 MHz, C₆D₆) δ 0.78 (d, *J* = 6.8 Hz, 3H); (0.78 (d, *J* = 6.8 Hz, 3H)); 0.84 (d, *J* = 6.8 Hz, 3H); (0.84 (d, *J* = 6.8 Hz, 3H)); 1.34–1.53 (m, 1H); (1.90–2.01 (dd, *J* = 2.4 and 17.1 Hz, 1H)); 1.91–2.29 (m, 3H); 2.43–2.52 (m, 1H); 2.74 (dd, *J* = 7.6 and 16.4 Hz, 1H); (2.76 (dd, *J* = 7.6 and 16.4 Hz, 1H)); 3.55–3.67 (m, 1H); 5.41–5.51 (m, 1H); 6.92 (d, *J* = 8.5 Hz, 2H); (6.97 (d, *J* = 8.5 Hz, 2H)); 7.09–7.23 (m, 9H); 7.57–7.68 (m, 6H); 7.73 (d, *J* = 8.5 Hz, 2H); 7.75 (d, *J* = 8.5 Hz, 2H). ¹³C NMR (62.5 MHz, C₆D₆) δ 17.5; 18.5; 33.3; (47.6); 47.9; 53.4; (71.4); 71.6; 71.8; (71.9); 123.5; 127.0; (127.1); 127.8; 128.2; 130.5; (134.0); 134.0; 135.8; 147.6; 150.4; (150.4); (208.0); 208.1. HRMS (ESI TOF-MS): calcd for C₃₂H₃₃NO₃SiNa 562.2026; found 562.2052.

(1*SR*,5*RS*)-5-Hydroxy-1-(4-nitrophenyl)-1-(triphenylsilyloxy)heptan-3-one (**57b**) and (1*SR*,5*SR*)-5-Hydroxy-1-(4-nitrophenyl)-1-(triphenylsilyloxy)heptan-3-one (**58b**). The mixture of aldol adducts **57b** and **58b** (74%, 0.116 g, 0.22 mmol) was obtained as a pale yellow oil (67:33 diastereoselectivity) after purification by flash column chromatography (silica gel 200–400 mesh) using a mixture of hexane/dichloromethane/ethyl acetate (50:40:10) as the eluent. *R*_f 0.40 (hexane/CH₂Cl₂/EtOAc 50:40:10). ¹H NMR (250 MHz, C₆D₆) δ 0.82 (t, *J* = 7.4 Hz, 3H); 1.08–1.32 (m, 2H); (1.97 (dd, *J* = 2.8 and 17.2 Hz, 1H)); 1.99–2.25 (m, 3H); 2.35–2.40 (m, 1H); 2.70 (dd, *J* = 7.4 and 16.3 Hz, 1H); (2.72 (dd, *J* = 7.1 and 16.3 Hz, 1H)); 3.62–3.77 (m, 1H); 5.40–5.50 (m, 1H); 6.89 (d, *J* = 8.7 Hz, 2H); (6.91 (d, *J* = 8.4 Hz, 2H)); 7.09–7.23 (m, 9H); 7.58–7.67 (m, 6H); 7.73 (d, *J* = 8.7 Hz, 2H); (7.74 (d, *J* = 8.4 Hz, 2H)). ¹³C NMR (125 MHz, C₆D₆) δ (9.9); 9.9; (29.7); 29.7; (50.1); 50.4; 53.3; 68.6; (68.7); (71.4); 71.6; 123.5; 127.0; (127.1); 127.9; 128.2; 128.3; 130.5; (130.5); (134.0); 134.0; 135.8; 147.6; 150.4; (150.4); (207.5); 207.7. HRMS (ESI TOF-MS): calcd for C₃₁H₃₂NO₃Si 526.2050; found 526.2037.

(1*SR*,5*SR*)-1-Hydroxy-5-(4-nitrophenyl)-1-phenyl-5-(triphenylsilyloxy)pentan-3-one (**57e**) and (1*RS*,5*SR*)-1-Hydroxy-5-(4-nitrophenyl)-1-phenyl-5-(triphenylsilyloxy)pentan-3-one (**58e**). The mixture of aldol adducts **57e** and **58e** (78%, 0.141 g, 0.24 mmol) was obtained as a pale yellow oil (54:46 diastereoselectivity) after purification by flash column chromatography (silica gel 200–400 mesh) using a mixture of hexane/dichloromethane/ethyl acetate (50:40:10) as the eluent. *R*_f 0.60 (hexane/CH₂Cl₂/EtOAc 50:40:10). ¹H NMR (250 MHz, C₆D₆) δ 2.12–2.55 (m, 3H); 2.60–2.80 (m, 2H); 4.87–4.97 (m, 1H); 5.39–5.49 (m, 1H); 6.85 (d, *J* = 8.7 Hz, 2H); (6.87 (d, *J* = 8.7 Hz, 2H)); 7.03–7.33 (m, 9H); 7.56–7.68 (m, 6H); 7.71 (d, *J* = 8.7 Hz, 2H). ¹³C NMR (125 MHz, C₆D₆) δ 30.0; (30.2); (52.7); 52.8; (53.3); 53.3; 69.7; (69.8); (71.4); 71.5; 123.5; 125.8; (125.9); 127.0; (127.1); 128.2; (128.5); 128.6; 130.5; (133.9); 134.0; 135.8; (143.6); 143.7; 147.5; 150.3; (206.7); 207.0. HRMS (ESI TOF-MS): calcd for C₃₅H₃₀NO₄Si 556.1944; found 556.1977.

(2*SR*,6*RS*)-2-(*tert*-Butyldimethylsilyloxy)-6-hydroxy-7-methyl-1,1,1-triphenyloctan-4-one (**68a**). The aldol adduct **68a** (95%, 54 mg, 0.10 mmol) was obtained as a white solid (>95:05 diastereoselectivity) after purification by flash column chromatography (silica gel 200–400 mesh) using a mixture of hexane/ethyl acetate (80:20) as the eluent. *R*_f 0.68 (20% EtOAc in hexane). Mp 89–91 °C. IR (neat) 3556, 3090, 3057, 3036, 3020, 2959, 2930, 2895, 2856, 1705, 1597, 1495, 1472, 1447, 1389, 1362, 1265, 1099, 1036, 1003, 957, 910,

895, 837, 777, 741, 704, 633 cm⁻¹. ¹H NMR (400 MHz; C₆D₆) δ 0.05 (s, 3H); 0.06 (s, 3H); 0.74 (d, *J* = 6.8 Hz, 3H); 0.75 (s, 9H); 0.79 (d, *J* = 6.8 Hz, 3H); 1.31–1.41 (m, 1H); 1.82 (d, *J* = 17.6 Hz, 1H); 1.92 (dd, *J* = 9.5 and 17.6 Hz, 1H); 2.05 (dd, *J* = 7.0 and 19.2 Hz, 1H); 2.82 (d, *J* = 19.2 Hz, 1H); 2.94 (br s, 1H); 3.67–3.71 (m, 1H); 6.36 (d, *J* = 7.0 Hz, 3H); 6.92 (br s, 3H); 7.06 (br s, 6H); 7.50 (br s, 6H). ¹³C NMR (62.5 MHz; C₆D₆) δ -5.3; -4.0; 17.3; 18.4; 18.7; 26.0; 33.2; 47.3; 51.6; 62.5; 70.5; 71.8; 126.3; 129.5; 132.5; 147.2; 210.5. HRMS (ESI TOF-MS): calcd for C₃₃H₄₄O₃SiNa 539.2957; found 539.2933.

(2*SR*,6*RS*)-2-(*tert*-Butyldimethylsilyloxy)-6-hydroxy-1,1,1-triphenyloctan-4-one (**68b**). The aldol adduct **68b** (92%, 51 mg, 0.10 mmol) was obtained as a white solid (>95:05 diastereoselectivity) after purification by flash column chromatography (silica gel 200–400 mesh) using a mixture of hexane/ethyl acetate (80:20) as the eluent. *R*_f 0.57 (20% EtOAc in hexane). Mp 145–148 °C. IR (neat) 3599, 3053, 3036, 2959, 2928, 2897, 2854, 1699, 1597, 1495, 1470, 1448, 1389, 1360, 1265, 1176, 1130, 1036, 999, 953, 833, 779, 743, 706, 629 cm⁻¹. ¹H NMR (500 MHz; C₆D₆) δ 0.04 (s, 3H); 0.05 (s, 3H); 0.75 (s, 9H); 0.82 (t, *J* = 7.5 Hz, 3H); 1.06–1.14 (m, 1H); 1.19–1.28 (m, 1H); 1.68 (dd, *J* = 2.7 and 17.8 Hz, 1H); 1.80 (dd, *J* = 9.3 and 17.8 Hz, 1H); 1.98 (dd, *J* = 7.0 and 19.3 Hz, 1H); 2.76 (d, *J* = 19.3 Hz, 1H); 2.81 (br s, 1H); 3.70–3.78 (m, 1H); 6.34 (d, *J* = 7.0 Hz, 1H); 6.92 (br s, 3H); 7.06 (br s, 6H); 7.50 (br s, 6H). ¹³C NMR (100 MHz; C₆D₆) δ -5.3; -4.0; 9.8; 18.4; 25.9; 29.6; 49.6; 51.5; 62.4; 68.6; 70.3; 126.2; 129.4; 132.8; 147.2; 210.2. HRMS (ESI TOF-MS): calcd for C₃₂H₄₂O₃SiNa 525.2801; found 525.2835.

(2*SR*,6*RS*)-2-(*tert*-Butyldimethylsilyloxy)-6-hydroxy-7,7-dimethyl-1,1,1-triphenyloctan-4-one (**68c**). The aldol adduct **68c** (98%, 57 mg, 0.11 mmol) was obtained as a white solid (>95:05 diastereoselectivity) after purification by flash column chromatography (silica gel 200–400 mesh) using a mixture of hexane/ethyl acetate (80:20) as the eluent. *R*_f 0.73 (20% EtOAc in hexane). Mp 181–184 °C. IR (neat) 3589, 3090, 3059, 3032, 3018, 2951, 2932, 2903, 2857, 1709, 1597, 1582, 1495, 1470, 1447, 1398, 1366, 1304, 1265, 1252, 1186, 1113, 1088, 1036, 1007, 955, 918, 835, 777, 739, 702, 631 cm⁻¹. ¹H NMR (500 MHz; C₆D₆) δ 0.04 (s, 3H); 0.08 (s, 3H); 0.74 (s, 9H); 0.76 (s, 9H); 1.99 (dd, *J* = 9.5 and 17.8 Hz, 1H); 2.05 (dd, *J* = 3.0 and 17.8 Hz, 1H); 2.12 (dd, *J* = 6.8 and 19.1 Hz, 1H); 2.88 (d, *J* = 19.1 Hz, 1H); 3.08 (d, *J* = 3.0 Hz, 1H); 3.66 (dt, *J* = 3.0 and 9.5 Hz, 1H); 6.38 (d, *J* = 6.8 Hz, 1H); 6.94 (br s, 3H); 7.08 (br s, 6H); 7.50 (br s, 6H). ¹³C NMR (62.5 MHz; C₆D₆) δ -5.3; -4.0; 18.4; 25.6; 26.0; 34.1; 45.2; 51.6; 62.4; 70.7; 74.5; 126.3; 129.4; 132.2; 147.1; 211.0. HRMS (ESI TOF-MS): calcd for C₃₄H₄₆O₃SiNa 553.3114; found 553.3110.

(2*SR*,6*RS*)-2-(*tert*-Butyldimethylsilyloxy)-6-hydroxy-7-methyl-1,1,1-triphenyloct-7-en-4-one (**68d**). The aldol adduct **68d** (94%, 53 mg, 0.10 mmol) was obtained as a white solid (>95:05 diastereoselectivity) after purification by flash column chromatography (silica gel 200–400 mesh) using a mixture of hexane/ethyl acetate (80:20) as the eluent. *R*_f 0.48 (20% EtOAc in hexane). Mp 65–67 °C. IR (neat) 3501, 3090, 3057, 3034, 3020, 2953, 2928, 2897, 2856, 1707, 1653, 1597, 1495, 1472, 1447, 1394, 1362, 1265, 1105, 1036, 1003, 951, 906, 837, 775, 741, 704, 631 cm⁻¹. ¹H NMR (500 MHz; C₆D₆) δ 0.06 (s, 3H); 0.07 (s, 3H); 0.75 (s, 9H); 1.49 (s, 3H); 1.94 (dd, *J* = 2.9 and 17.4 Hz, 1H); 2.04 (dd, *J* = 6.4 and 19.2 Hz, 1H); 2.06 (dd, *J* = 9.4 and 17.4 Hz, 1H); 2.65 (d, *J* = 2.9 Hz, 1H); 2.82 (d, *J* = 19.2 Hz, 1H); 4.38 (d, *J* = 9.4 Hz, 1H); 4.71–4.72 (m, 1H); 4.88–4.89 (m, 1H); 6.36 (d, *J* = 6.4 Hz, 1H); 6.93 (br s, 3H); 7.07 (br s, 6H); 7.51 (br s, 6H). ¹³C NMR (62.5 MHz; C₆D₆) δ -5.2; -4.0; 18.1; 18.4; 26.0; 48.6; 51.7; 62.5; 70.4; 71.1; 110.9; 126.3; 129.5; 132.5; 146.2; 146.9; 209.3. HRMS (ESI TOF-MS): calcd for C₃₃H₄₃O₃Si 515.2982; found 515.2953.

(1*RS*,5*SR*)-5-(*tert*-Butyldimethylsilyloxy)-1-hydroxy-1,6,6,6-tetraphenylhexan-3-one (**68e**) and (1*SR*,5*SR*)-5-(*tert*-Butyldimethylsilyloxy)-1-hydroxy-1,6,6,6-tetraphenylhexan-3-one (**69e**). The mixture of aldol adducts **68e** and **69e** (89%, 54 mg, 0.10 mmol) was obtained as a white solid (91:09 diastereoselectivity) after purification by flash column chromatography (silica gel 200–400 mesh) using a mixture of hexane/ethyl acetate (80:20) as the eluent. *R*_f 0.50 (20% EtOAc in hexane). Mp 87–89 °C. IR (neat) 3499, 3090, 3057, 3034, 2955, 2930, 2897, 2856, 1707, 1597, 1495, 1472, 1448, 1391, 1362, 1265,

1103, 1036, 953, 837, 775, 741, 704, 633 cm^{-1} . ^1H NMR (500 MHz; C_6D_6) δ (0.05 (s, 3H)); 0.06 (s, 3H); (0.06 (s, 3H)); 0.07 (s, 3H); (0.75 (s, 9H)); 0.76 (s, 9H); 1.91–2.01 (m, 2H); 2.16 (dd, J = 9.2 and 17.8 Hz, 1H); 2.72 (d, J = 19.0 Hz, 1H); (2.72 (d, J = 19.0 Hz, 1H)); (2.91 (d, J = 2.5 Hz, 1H)); 3.00 (d, J = 2.5 Hz, 1H); 4.96 (dt, J = 2.5 and 9.2 Hz, 1H); (5.04–5.06 (m, 1H)); 6.34 (d, J = 6.4 Hz, 1H); 6.95–7.52 (m, 20H). ^{13}C NMR (62.5 MHz; C_6D_6) δ –5.3; (–4.2); –4.0; 18.4; 26.0; 51.5; (51.9); 52.1; (62.3); 62.4; 69.8; (69.9); 70.3; (70.5); (126.0); 126.1; 126.2; 127.5; 128.5; 129.4; 132.7; 143.5; (143.7); 147.0; 209.3. HRMS (ESI TOF-MS): calcd for $\text{C}_{36}\text{H}_{43}\text{O}_3\text{Si}$ 551.2982; found 551.3027.

(1*SR*,5*SR*)-5-(*tert*-Butyldimethylsilyloxy)-1-hydroxy-1-(4-nitrophenyl)-6,6,6-triphenylhexan-3-one (**68f**). The aldol adduct **68f** (84%, 55 mg, 0.09 mmol) was obtained as a white solid (>95:05 diastereoselectivity) after purification by flash column chromatography (silica gel 200–400 mesh) using a mixture of hexane/ethyl acetate (80:20) as the eluent. R_f 0.17 (20% EtOAc in hexane). Mp 174–177 °C. IR (neat) 3472, 3055, 2986, 2957, 2930, 2897, 2854, 1707, 1599, 1522, 1495, 1447, 1389, 1348, 1265, 1194, 1165, 1097, 1038, 987, 951, 897, 852, 837, 741, 706 cm^{-1} . ^1H NMR (400 MHz; CDCl_3) δ –0.11 (s, 3H); –0.03 (s, 3H); 0.61 (s, 9H); 1.98 (dd, J = 6.9 and 19.4 Hz, 1H); 2.60 (dd, J = 9.2 and 18.1 Hz, 1H); 2.70 (dd, J = 2.9 and 18.1 Hz, 1H); 2.80 (d, J = 19.4 Hz, 1H); 3.68 (d, J = 2.9 Hz, 1H); 5.28 (d, J = 9.2 Hz, 1H); 6.11 (d, J = 6.9 Hz, 1H); 7.00–7.46 (m, 15H); 7.50 (d, J = 8.8 Hz, 1H); 8.18 (d, J = 8.8 Hz, 1H). ^{13}C NMR (100 MHz; CDCl_3) δ –5.6; –4.3; 18.1; 25.6; 51.3; 51.4; 61.9; 68.9; 69.7; 123.7; 126.0; 126.4; 127.8; 128.9; 146.4; 147.3; 149.7; 209.2. HRMS (ESI TOF-MS): calcd for $\text{C}_{36}\text{H}_{41}\text{NO}_3\text{SiNa}$ 618.2652; found 618.2668.

(1*SR*,5*SR*)-5-(*tert*-Butyldimethylsilyloxy)-1-hydroxy-1-(4-methoxyphenyl)-6,6,6-triphenylhexan-3-one (**68g**) and (1*SR*,5*SR*)-5-(*tert*-Butyldimethylsilyloxy)-1-hydroxy-1-(4-methoxyphenyl)-6,6,6-triphenylhexan-3-one (**69g**). The mixture of aldol adducts **68g** and **69g** (78%, 50 mg, 0.09 mmol) was obtained as a yellow oil (91:09 diastereoselectivity) after purification by flash column chromatography (silica gel 200–400 mesh) using a mixture of hexane/ethyl acetate (80:20) as the eluent. R_f 0.43 (20% EtOAc in hexane). IR (neat) 3483, 3090, 3057, 3034, 3020, 2955, 2928, 2901, 2854, 1707, 1612, 1514, 1495, 1472, 1464, 1447, 1396, 1304, 1250, 1175, 1101, 1036, 953, 835, 775, 739, 704, 633 cm^{-1} . ^1H NMR (500 MHz; C_6D_6) δ (0.06 (s, 3H)); 0.07 (s, 3H); 0.08 (s, 3H); (0.74 (s, 9H)); 0.76 (s, 9H); 1.98 (dd, J = 6.8 and 19.3 Hz, 1H); 2.06 (dd, J = 3.4 and 17.2 Hz, 1H); 2.25 (dd, J = 9.2 and 17.2 Hz, 1H); 2.71 (d, J = 19.3 Hz, 1H); (2.76 (d, J = 19.3 Hz, 1H)); 2.89 (br s, 1H); 3.33 (s, 3H); (3.34 (s, 3H)); 4.96 (dd, J = 3.4 and 9.2 Hz, 1H); (5.05 (dd, J = 1.5 and 8.8 Hz, 1H)); 6.34 (d, J = 6.8 Hz, 1H); 6.76 (dt, J = 2.2 and 8.8 Hz, 1H); 6.93 (br s, 3H); 7.06 (dt, J = 2.2 and 8.8 Hz, 1H); 7.19 (br s, 6H); 7.51 (br s, 6H). ^{13}C NMR (62.5 MHz; C_6D_6) δ –5.2; (–4.1); –4.0; 18.4; 26.0; 51.6; (52.1); (52.1); 52.3; 54.8; (62.3); 62.4; 69.6; (69.7); 70.3; (70.5); 113.9; 126.2; (127.2); 127.4; 129.4; 132.7; 135.7; (135.8); 147.1; 159.5; 209.2 (209.3). HRMS (ESI TOF-MS): calcd for $\text{C}_{37}\text{H}_{43}\text{O}_3\text{Si}$ 563.2982; found 563.2946.

Stereochemistry proofs. (3*R*,7*S*)-3,7-Dihydroxy-2,2,8,8-tetramethylnonan-5-one (**35**) and (3*R*,7*R*)-3,7-Dihydroxy-2,2,8,8-tetramethylnonan-5-one (**36**). Aldol adducts **53c** and **54c** (12 mg, 0.02 mmol) were dissolved in 1.0 mL of acetonitrile at 0 °C. To the resulting solution were added four drops of aqueous 48% HF solution. The mixture was stirred for 5 min at 0 °C, then for 1.5 h at room temperature. The reaction was quenched by the addition of solid NaHCO_3 , filtered, and concentrated under reduced pressure to give 6 mg (100%) of **35** and **36** as a yellow solid. R_f 0.38 (20% EtOAc in hexane). ^1H NMR (250 MHz; C_6D_6) δ (0.86 (s, 18H)); 0.87 (s, 18H); 2.10–2.19 (m, 2H); 2.23–2.35 (m, 2H); (2.90 (br s, 2H)); 3.09 (br s, 2H); 3.67–3.73 (m, 2H). ^{13}C NMR (62.5 MHz; C_6D_6) δ 25.8; (34.3); 34.4; (45.4); 45.7; (74.9); 75.2; (213.1); 213.5.

(1*SR*,5*SR*)-1,5-Dihydroxy-6-methyl-1-(4-nitrophenyl)heptan-3-one (**59**) and (1*SR*,5*SR*)-1,5-Dihydroxy-6-methyl-1-(4-nitrophenyl)heptan-3-one (**60**). The inseparable aldol adduct **61a** and **62a** (50 mg, 0.093 mmol) was dissolved in $\text{MeCN}/\text{CH}_2\text{Cl}_2$ 1:1 (4.0 mL) at 0 °C. Four drops of aqueous 48% HF solution were added to the resulting solution. The mixture was stirred for 5 min at 0 °C, then for 3 h at room temperature. The reaction was quenched by the addition of solid

NaHCO_3 , filtered, and concentrated under reduced pressure to give 26 mg (99%) of diols **59** and **60** as a yellow solid. R_f 0.38 (20% EtOAc in hexane). (1*SR*,5*SR*)-1,5-Dihydroxy-6-methyl-1-(4-nitrophenyl)heptan-3-one (**59**): ^1H NMR (500 MHz; C_6D_6) δ 0.78 (d, J = 6.8 Hz, 3H); 0.83 (d, J = 6.8 Hz, 3H); 1.34–1.54 (m, 1H); 1.97 (dd, J = 2.5 and 16.4 Hz, 1H); 2.10 (dd, J = 3.0 and 17.1 Hz, 1H); 2.21 (dd, J = 9.8 and 16.4 Hz, 1H); 2.28 (dd, J = 9.6 and 17.1 Hz, 1H); 2.59 (br s, 1H); 3.41 (br s, 1H); 3.63–3.75 (m, 1H); 4.90 (dd, J = 3.0 and 9.6 Hz, 1H); 6.99 (d, J = 8.5 Hz, 2H); 7.90 (d, J = 8.5 Hz, 2H). (1*SR*,5*SR*)-1,5-Dihydroxy-6-methyl-1-(4-nitrophenyl)heptan-3-one (**60**): ^1H NMR (500 MHz; C_6D_6) δ 0.79 (d, J = 6.8 Hz, 3H); 0.84 (d, J = 6.8 Hz, 3H); 1.34–1.54 (m, 1H); 1.99 (dd, J = 2.4 and 16.6 Hz, 1H); 2.09 (dd, J = 2.9 and 17.2 Hz, 1H); 2.17 (dd, J = 9.3 and 16.6 Hz, 1H); 2.39 (dd, J = 9.6 and 17.2 Hz, 1H); 2.59 (br s, 1H); 3.41 (br s, 1H); 3.63–3.75 (m, 1H); 4.84–4.94 (m, 1H); 7.01 (d, J = 8.5 Hz, 2H); 7.90 (d, J = 8.5 Hz, 2H).

(2*SR*,4*SR*,6*SR*)-2-(*tert*-Butyldimethylsilyloxy)-1,1,1-triphenyloctane-4,6-diol (**70**). To a solution of aldol adduct **68b** (100 mg, 0.20 mmol) in THF/MeOH 4:1 (1.0 mL) at –60 °C was added Et_2BOMe (0.10 mL, 0.72 mmol) dropwise, and the resulting solution was stirred for 15 min. A solution of LiBH_4 (0.36 mL, 0.72 mmol, 2.0 M in THF) was added dropwise, and the resulting solution was stirred for 2 h at –60 °C. The mixture was allowed to warm to –40 °C, and the reaction was then quenched by the addition of pH 7.0 aqueous phosphate buffer solution (8 mL). Then, MeOH (15 mL) and H_2O_2 30% (6 mL) were added dropwise at 0 °C. The resulting mixture was stirred for 1 h at 0 °C, after which MeOH was removed by reduced pressure. The solution was diluted with H_2O (10 mL), the phases were separated, and the aqueous phase was extracted with EtOAc (4 \times 30 mL). The organic phase was washed with water (2 \times 25 mL) and brine (2 \times 25 mL), dried over MgSO_4 , filtered, and concentrated under reduced pressure. The residue was purified by flash column chromatography (silica gel 200–400 mesh) using a mixture of hexane/ethyl acetate (80:20) as the eluent, which provided 84 mg (84%, dr > 95:05) of **70** as a colorless oil. R_f 0.36 (20% EtOAc in hexane). IR (neat) 3387, 3090, 3057, 3034, 3020, 2959, 2930, 2856, 1597, 1495, 1472, 1464, 1447, 1265, 1136, 1103, 1036, 1003, 945, 905, 835, 775, 741, 706 cm^{-1} . ^1H NMR (250 MHz; C_6D_6) δ –0.08 (s, 3H); 0.25 (s, 3H); 0.81 (t, J = 7.6 Hz, 3H); 0.85 (s, 9H); 1.23–1.53 (m, 5H); 2.07 (ddd, J = 2.8; 6.6 and 14.7 Hz, 1H); 2.51 (br s, 1H); 3.04 (br s, 1H); 3.47–3.55 (m, 1H); 3.87–3.95 (m, 1H); 5.56 (dd, J = 2.8 and 5.7 Hz, 2H); 7.01 (t, J = 7.5 Hz, 3H); 7.13 (t, J = 7.5 Hz, 6H); 7.54 (d, J = 7.5 Hz, 6H). ^{13}C NMR (62.5 MHz; C_6D_6) δ –4.3; –3.5; 9.7; 18.8; 26.4; 31.3; 42.9; 45.6; 64.0; 71.2; 74.1; 74.4; 126.2; 127.7; 130.9; 145.9. HRMS (ESI TOF-MS): calcd for $\text{C}_{32}\text{H}_{44}\text{O}_3\text{SiNa}$ 527.2957; found 527.2989.

tert-Butyl((1*SR*)-3-((4*SR*,6*SR*)-6-ethyl-2,2-dimethyl-1,3-dioxan-4-yl)-1,1,1-triphenylpropan-2-yloxy)dimethylsilane (**71**). PPTS was added in catalytic amounts at room temperature to a solution of diol **70** (19 mg, 0.04 mmol) in 2,2-dimethoxypropane (1.0 mL). The reaction mixture was stirred for 2 h and quenched by the addition of solid NaHCO_3 , filtered, and concentrated under reduced pressure to give 20 mg (95%) of **71** as a yellow oil. R_f 0.79 (20% EtOAc in hexane). IR (neat) 3090, 3057, 3034, 2993, 2961, 2935, 2856, 1597, 1493, 1464, 1448, 1381, 1265, 1202, 1169, 1146, 1107, 1034, 1003, 959, 835, 775, 744, 706 cm^{-1} . ^1H NMR (250 MHz; C_6D_6) δ –0.03 (s, 3H); 0.24 (s, 3H); 0.84 (s, 9H); 0.92 (t, J = 7.4 Hz, 3H); 1.06–1.66 (m, 5H); 1.30 (s, 3H); 1.51 (s, 3H); 2.21 (ddd, J = 3.6; 6.5 and 15.0 Hz, 1H); 3.48–3.58 (m, 1H); 3.62–3.73 (m, 1H); 5.47 (t, J = 4.5 Hz, 1H); 7.00 (t, J = 7.4 Hz, 3H); 7.11 (t, J = 7.4 Hz, 6H); 7.52 (d, J = 7.4 Hz, 6H). ^{13}C NMR (62.5 MHz; C_6D_6) δ –4.5; –3.5; 9.6; 18.7; 20.2; 26.3; 29.7; 30.5; 37.5; 44.2; 64.0; 68.0; 70.3; 73.3; 98.6; 126.2; 127.7; 131.1; 145.6. HRMS (EI TOF-MS): calcd for $\text{C}_{34}\text{H}_{45}\text{O}_3\text{Si}$ [M – CH_3] $^+$ 529.3138; found 529.3130.

(2*SR*,4*SR*,6*SR*)-1,1,1-Triphenyloctane-2,4,6-triol (**72**). Four drops of aqueous 48% HF solution were added at 0 °C to a solution of diol **70** (20 mg, 0.04 mmol) in acetonitrile (0.5 mL). The mixture was stirred for 5 min at 0 °C for 2 days at room temperature and quenched by the addition of solid NaHCO_3 . The solution was then filtered and concentrated under reduced pressure to give 16 mg (100%) of **72** as a

colorless oil. R_f 0.36 (20% EtOAc in hexane). IR (neat) 3429, 3088, 3057, 2962, 2928, 2876, 2854, 1597, 1495, 1447, 1441, 1265, 1134, 1097, 1036, 845, 739, 702 cm^{-1} . ^1H NMR (250 MHz; CD_3OD) δ 0.92 (t, J = 7.4 Hz, 3H); 1.36–1.71 (m, 5H); 1.86 (dd, J = 4.7 and 14.4 Hz, 1H); 3.59–3.69 (m, 1H); 4.10–4.20 (m, 1H); 5.50 (d, J = 9.6 Hz, 1H); 7.14 (t, J = 7.0 Hz, 3H); 7.23 (t, J = 7.0 Hz, 6H); 7.33 (d, J = 7.0 Hz, 6H). ^{13}C NMR (62.5 MHz; CD_3OD) δ 10.1; 31.2; 42.1; 44.4; 63.3; 71.8; 72.9; 73.6; 127.0; 128.6; 131.3; 146.6. HRMS (ESI TOF-MS): calcd for $\text{C}_{26}\text{H}_{30}\text{O}_3\text{Na}$ 413.2093; found 413.2098.

(2*SR*,4*RS*,6*SR*)-2-(*tert*-Butyldimethylsilyloxy)-1,1,1-triphenyloctane-4,6-diol (**73**) and (2*SR*,4*SR*,6*SR*)-2-(*tert*-Butyldimethylsilyloxy)-1,1,1-triphenyloctane-4,6-diol (**70**). Acetic acid (0.6 mL) was added to a stirring suspension of $\text{Me}_4\text{NHB}(\text{OAc})_3$ (422 mg, 1.6 mmol) in THF (0.6 mL) at room temperature. The resulting mixture was stirred for 30 min and was cooled to -40°C . The aldol adduct **68b** (100 mg, 0.20 mmol) in THF (0.6 mL) was added via cannula. Then, a solution of CSA (23 mg, 0.10 mmol) in acetic acid/THF 1:1 (1.2 mL) was added, and the mixture was stirred for 3 days at -22°C . The reaction was quenched by the addition of a saturated aqueous solution of NaHCO_3 (15 mL) followed by the addition of a potassium tartrate aqueous solution (15 mL) and Et_2O (50 mL). The mixture was stirred vigorously at room temperature for 8 h. The phases were separated, and the aqueous phase was extracted with Et_2O (4×20 mL). The organic phase was washed with brine (2×25 mL), dried over MgSO_4 , filtered, and concentrated under reduced pressure. The residue was purified by flash column chromatography (silica gel 200–400 mesh) using a mixture of hexane/ethyl acetate (80:20) as the eluent, which provided 53 mg of **73** and **70** (50%, dr = 35:65, **73**:**70**) as a colorless oil. R_f 0.36 (20% EtOAc in hexane). IR (neat) 3393, 3090, 3057, 3034, 3020, 2959, 2930, 2856, 1597, 1495, 1472, 1462, 1447, 1256, 1101, 1036, 1003, 947, 833, 773, 743, 704 cm^{-1} . ^1H NMR (250 MHz; C_6D_6) δ (−0.29 (s, 3H)); −0.08 (s, 3H); 0.25 (s, 3H); (0.32 (s, 3H)); (0.62 (t, J = 7.3 Hz, 3H)); 0.81 (t, J = 7.6 Hz, 3H); 0.85 (s, 9H); (0.88 (s, 9H)); 0.99–1.58 (m, 5H); 2.07 (ddd, J = 2.8; 6.6 and 14.7 Hz, 1H); (2.19–2.29 (m, 1H)); (3.34–3.43 (m, 1H)); 3.47–3.55 (m, 1H); 3.85–3.96 (m, 1H); (4.35 (t, J = 9.1 Hz, 1H)); 5.56 (dd, J = 2.8 and 5.7 Hz, 2H); (6.07 (d, J = 8.5 Hz, 1H)); 7.01 (t, J = 7.5 Hz, 3H); 7.13 (t, J = 7.5 Hz, 6H); 7.52 (d, J = 7.5 Hz, 6H) (7.72 (d, J = 6.8 Hz, 6H)). ^{13}C NMR (62.5 MHz; C_6D_6) δ (−4.4); −4.3; (−4.3); −3.5; 9.7; (10.1); 18.8; (19.1); 26.4; (26.5); (30.1); 31.3; (42.5); 42.9; (44.2); 45.6; (62.9); 64.0; (66.0); 71.3; (71.4); (73.6); 74.1; 74.4; (126.0); 126.2; 127.7; 131.0; 145.8. HRMS (ESI TOF-MS): calcd for $\text{C}_{32}\text{H}_{44}\text{O}_3\text{SiNa}$ 527.2957; found 527.2936.

tert-Butyl((*SR*)-3-((4*RS*,6*SR*)-6-ethyl-2,2-dimethyl-1,3-dioxan-4-yl)-1,1,1-triphenylpropan-2-yloxy)dimethylsilane (**74**) and *tert*-Butyl((*SR*)-3-((4*SR*,6*SR*)-6-ethyl-2,2-dimethyl-1,3-dioxan-4-yl)-1,1,1-triphenylpropan-2-yloxy)dimethylsilane (**71**). PPTS was added in catalytic amounts at room temperature to a solution of a mixture of diols **73** and **70** (10 mg, 0.02 mmol) in 2,2-dimethoxypropane (0.5 mL). The reaction mixture was stirred for 2 h, quenched by the addition of solid NaHCO_3 , filtered, and concentrated under reduced pressure to give 11 mg (95%) of **74** and **71** as a yellow oil. R_f 0.79 (10% EtOAc in hexane). IR (neat) 3090, 3055, 2986, 2961, 2932, 2856, 1597, 1495, 1472, 1464, 1447, 1379, 1265, 1233, 1202, 1171, 1107, 1034, 1003, 960, 833, 741, 706 cm^{-1} . ^1H NMR (400 MHz; C_6D_6) δ (−0.37 (s, 3H)); −0.03 (s, 3H); (0.21 (s, 3H)); 0.24 (s, 3H); (0.81 (t, J = 7.5 Hz, 3H)); (0.83 (s, 9H)); 0.84 (s, 9H); 0.92 (t, J = 7.4 Hz, 3H); 1.09–1.65 (m, 5H); 1.30 (s, 3H); 1.51 (s, 3H); (1.53 (s, 3H)); (1.62 (s, 3H)); 2.16–2.24 (m, 1H); 3.48–3.56 (m, 1H); 3.64–3.71 (m, 1H); (4.20–4.27 (m, 1H)); 5.48 (dd, J = 4.0 and 5.0 Hz, 1H); (5.74 (d, J = 8.0 Hz, 1H)); 7.01 (t, J = 7.4 Hz, 3H); 7.11 (t, J = 7.4 Hz, 6H); 7.53 (d, J = 7.4 Hz, 6H) (7.67 (br s, 6H)). ^{13}C NMR (100 MHz; C_6D_6) δ (−4.7); −4.5; (−4.3); −3.5; 9.6; (9.8); 18.7; (19.0); 20.1; (25.7); (26.2); 26.3; (26.6); (29.1); 29.7; 30.5; 37.5; (38.1); 44.2; (44.7); (62.9); 64.0; (64.8); 68.0; (68.1); 70.3; 73.3; (74.3); 98.6; (99.9); (125.8); 126.2; 127.9; 131.1; 145.5. HRMS (EI TOF-MS): calcd for $\text{C}_{34}\text{H}_{45}\text{O}_3\text{Si}$ [M − CH_3] $^+$ 529.3138; found 529.3147.

(2*SR*,4*RS*,6*SR*)-1,1,1-Triphenyloctane-2,4,6-triol (**75**) and (2*SR*,4*SR*,6*SR*)-1,1,1-Triphenyloctane-2,4,6-triol (**72**). Eight drops of aqueous 48% HF solution were added at 0°C to a solution of

a mixture of diols **73** and **70** (24 mg, 0.05 mmol) in acetonitrile (1.2 mL). The mixture was stirred for 5 min at 0°C for 4 days at room temperature, quenched by the addition of solid NaHCO_3 , filtered, and concentrated under reduced pressure to give 21 mg (100%) of **75** and **72** as a colorless oil. R_f 0.36 (20% EtOAc in hexane). IR (neat) 3425, 3088, 3057, 2962, 2930, 1597, 1495, 1447, 1265, 1134, 1095, 1036, 895, 845, 739, 704 cm^{-1} . ^1H NMR (400 MHz; CD_3OD) δ 0.89–2.29 (m, 9H); 3.61–3.71 (m, 1H); 4.06–4.18 (m, 1H); 5.50 (d, J = 9.6 Hz, 1H); (5.65 (d, J = 10.0 Hz, 1H)); 7.13–7.16 (m, 3H); 7.21–7.24 (m, 6H); 7.32–7.37 (m, 6H). ^{13}C NMR (100 MHz; CD_3OD) δ 10.1; (10.3); 31.2; (31.7); 42.1; (43.7); 44.4; (45.6); (63.1); 63.3; (66.7); (70.8); (70.8); 71.7; 72.9; 73.6; (126.8); 126.9; 128.5; 131.2; 146.6. HRMS (ESI TOF-MS): calcd for $\text{C}_{26}\text{H}_{31}\text{O}_3$ 391.2273; found 391.2256.

■ ASSOCIATED CONTENT

● Supporting Information

^1H NMR, ^{13}C NMR, IR, and HRMS spectra for the prepared compounds and Cartesian coordinates of transition structures with gas-phase and solution-phase SCF absolute energies. This material is available free of charge via the Internet at <http://pubs.acs.org>.

■ AUTHOR INFORMATION

Corresponding Author

*E-mail: ldias@iqm.unicamp.br.

■ ACKNOWLEDGMENTS

We are grateful to FAEP-UNICAMP, FAPESP, CNPq and INCT-INOVAR (Proc. CNPq 573.564/2008-6) for financial support and to Prof. Carol H. Collins (IQ-UNICAMP) for helpful suggestions about English grammar and style.

■ REFERENCES

- (1) (a) Cowden, C. J.; Paterson, I. *Org. React.* **1997**, *51*, 1. (b) Franklin, A. S.; Paterson, I. *Contemp. Org. Synth.* **1994**, *1*, 317. (c) Heathcock, C. H. In *Comprehensive Organic Synthesis*; Heathcock, C. H., Ed.; Pergamon Press: New York, 1991; Vol. 2, p 181. (d) Kim, B. M.; Williams, S. F.; Masamune, S. In *Comprehensive Organic Synthesis*; Heathcock, C. H., Ed.; Pergamon Press: New York, 1991; Vol. 2, p 239. (e) Evans, D. A.; Nelson, J. V.; Taber, T. R. *Top. Stereochem.* **1982**, *13*, 1. (f) Dias, L. C.; Aguilar, A. M. *Chem. Soc. Rev.* **2008**, *37*, 451. (g) Dias, L. C.; Aguilar, A. M. *Quim. Nova* **2007**, *30*, 2007. (h) Schetter, B.; Mahrwald, R. *Angew. Chem., Int. Ed.* **2006**, *45*, 7506.
- (2) Blanchette, M. A.; Malamas, M. S.; Nantz, M. H.; Roberts, J. C.; Somfai, P.; Whritenour, D. C.; Masamune, S.; Kageyama, M.; Tamura, T. *J. Org. Chem.* **1989**, *54*, 2817.
- (3) (a) Paterson, I.; Oballa, R. M.; Norcross, R. D. *Tetrahedron Lett.* **1996**, *37*, 8581. (b) Paterson, I.; Gibson, K. R.; Oballa, R. M. *Tetrahedron Lett.* **1996**, *37*, 8585. (c) Paterson, I.; Collet, L. A. *Tetrahedron Lett.* **2001**, *42*, 1187. (d) Paterson, I.; Di Francesco, M. E.; Kuhn, T. *Org. Lett.* **2003**, *5*, 599. (e) Paterson, I.; Tudge, M. *Tetrahedron* **2003**, *59*, 6833. (f) Paterson, I.; Coster, M. J.; Chen, D. Y.-K.; Aceña, J. L.; Bach, J.; Keown, L. E.; Trieselmann, T. *Org. Biomol. Chem.* **2005**, *3*, 2420.
- (4) (a) Evans, D. A.; Gage, J. R. *Tetrahedron Lett.* **1990**, *31*, 6129. (b) Evans, D. A.; Coleman, P. J.; Côté, B. *J. Org. Chem.* **1997**, *62*, 788. (c) Evans, D. A.; Côté, B.; Coleman, P. J.; Connell, B. T. *J. Am. Chem. Soc.* **2003**, *125*, 10893. (d) Evans, D. A.; Connell, B. T. *J. Am. Chem. Soc.* **2003**, *125*, 10899. (e) Evans, D. A.; Nagorny, P.; McRae, K. J.; Sonntag, L.-S.; Reynolds, D. J.; Vounatsos, F. *Angew. Chem., Int. Ed.* **2007**, *46*, 545. (f) Evans, D. A.; Welch, D. E.; Speed, A. W. H.; Moniz, G. A.; Reichelt, A.; Ho, S. *J. Am. Chem. Soc.* **2009**, *131*, 3840.
- (5) (a) Denmark, S. E.; Fujimori, S.; Pham, S. M. *J. Org. Chem.* **2005**, *70*, 10823. (b) Denmark, S. E.; Fujimori, S. *Synlett* **2001**, 1024. (c) Denmark, S. E.; Fujimori, S. *J. Am. Chem. Soc.* **2005**, *127*, 8971.

- (6) (a) Dias, L. C.; Baú, R. Z.; de Sousa, M. A.; Zukerman-Schpector, J. *Org. Lett.* **2002**, *4*, 4325. (b) Dias, L. C.; Aguilar, A. M. *Org. Lett.* **2006**, *8*, 4629. (c) Dias, L. C.; Marchi, A. A.; Ferreira, M. A. B.; Aguilar, A. M. *Org. Lett.* **2007**, *9*, 4869. (d) Dias, L. C.; Marchi, A. A.; Ferreira, M. A. B.; Aguilar, A. M. *J. Org. Chem.* **2008**, *73*, 6299. (e) Dias, L. C.; Pinheiro, S. M.; Oliveira, V. M.; Ferreira, M. A. B.; Tormena, C. F.; Aguilar, A. M.; Zukerman-Schpector, J.; Tiekink, E. R. *Tetrahedron* **2009**, *65*, 8714. (f) Dias, L. C.; Aguilar, A. M.; Salles, A. G. Jr.; Steil, L. J.; Roush, W. R. *J. Org. Chem.* **2005**, *70*, 10461. (g) Dias, L. C.; Salles, A. G. Jr. *Tetrahedron Lett.* **2006**, *47*, 2213.
- (7) (a) Arefolov, A.; Panek, J. S. *Org. Lett.* **2002**, *4*, 2397. (b) Park, P. K.; O'Malley, S. J.; Schmidt, D. R.; Leighton, J. L. *J. Am. Chem. Soc.* **2006**, *128*, 2796. (c) Li, P.; Li, J.; Arian, F.; Ahlbrecht, W.; Dieckmann, M.; Menche, D. *J. Am. Chem. Soc.* **2009**, *131*, 11678. (d) Li, P.; Li, J.; Arian, F.; Ahlbrecht, W.; Dieckmann, M.; Menche, D. *J. Org. Chem.* **2010**, *75*, 2429. (e) Fettes, A.; Carreira, E. M. *J. Org. Chem.* **2003**, *68*, 9274. (f) Zhang, Y.; Arpin, C. C.; Cullen, A. J.; Mitton-Fry, M. J.; Sammakia, T. *J. Org. Chem.* **2011**, *76*, 7641. For lithium-mediated aldol reactions employing β -alkoxy methylketones with super silyl protecting groups at the β -oxygen, see: (g) Yamaoka, Y.; Yamamoto, H. *J. Am. Chem. Soc.* **2010**, *132*, 5354. (h) Albert, B. J.; Yamaoka, Y.; Yamamoto, H. *Angew. Chem., Int. Ed.* **2011**, *50*, 2610.
- (8) (a) Paton, R. S.; Goodman, J. M. *Org. Lett.* **2006**, *8*, 4299. (b) Goodman, J. M.; Paton, R. S. *Chem. Commun.* **2007**, 2124. (c) Paton, R. S.; Goodman, J. M. *J. Org. Chem.* **2008**, *73*, 1253.
- (9) Dias, L. C.; de Lucca, E. C.; Ferreira, M. A. B.; Garcia, D. C.; Tormena, C. F. *Org. Lett.* **2010**, *12*, 5056.
- (10) (a) List, B. *Tetrahedron* **2002**, *58*, 5573. (b) List, B.; Pojarliev, P.; Castello, C. *Org. Lett.* **2001**, *3*, 573. (c) List, B.; Lerner, R. A.; Barbas, C. F. III *J. Am. Chem. Soc.* **2000**, *122*, 2395.
- (11) Doi, T.; Numajiri, Y.; Munakata, A.; Takahashi, T. *Org. Lett.* **2006**, *8*, 531.
- (12) Zou, B.; Wei, J.; Cai, G.; Ma, D. *Org. Lett.* **2003**, *5*, 3503.
- (13) (a) Burk, R. M.; Gac, T. S.; Roof, M. B. *Tetrahedron Lett.* **1994**, *35*, 8111. (b) Lundquist, J. T. IV; Satterfield, A. D.; Pelletier, J. C. *Org. Lett.* **2006**, *8*, 3915.
- (14) Davis, F. A.; Reddy, R. E.; Szewczyk, J. M.; Reddy, G. V.; Portonovo, P. S.; Zhang, H.; Fanelli, D.; Reddy, R. T.; Zhou, P.; Carroll, P. J. *J. Org. Chem.* **1997**, *62*, 2555.
- (15) (a) Dudnik, A. S.; Schwier, T.; Gevorgyan, V. *Org. Lett.* **2008**, *10*, 1465. (b) Dudnik, A. S.; Schwier, T.; Gevorgyan, V. *Tetrahedron* **2009**, *65*, 1859.
- (16) (a) Corey, E. J.; Cho, H.; Rucker, C.; Hua, D. H. *Tetrahedron Lett.* **1981**, *22*, 3455. (b) Dias, L. C.; Finelli, F. G.; Conejero, L. S.; Krogh, R.; Andricopulo, A. D. *Eur. J. Org. Chem.* **2010**, 6748.
- (17) (a) Kobayashi, Y.; Tan, C.-H.; Kishi, Y. *Helv. Chim. Acta* **2000**, *83*, 2562. (b) Kobayashi, Y.; Lee, J.; Tezuka, K.; Kishi, Y. *Org. Lett.* **1999**, *1*, 2177.
- (18) (a) Narasaka, K.; Pai, F.-C. *Chem. Lett.* **1980**, 1415. (b) Narasaka, K.; Pai, F.-C. *Tetrahedron* **1984**, *40*, 2233. (c) Paterson, I.; Norcross, R. D.; Ward, R. A.; Romea, P.; Lister, M. A. *J. Am. Chem. Soc.* **1994**, *116*, 11287.
- (19) (a) Rychnovsky, S. D.; Skaltitzky, D. J. *Tetrahedron Lett.* **1990**, *31*, 945. (b) Rychnovsky, S. D.; Rogers, B.; Yang, G. *J. Org. Chem.* **1993**, *58*, 3511. (c) Rychnovsky, S. D.; Rogers, B. N.; Richardson, T. I. *Acc. Chem. Res.* **1998**, *31*, 9. For a theoretical work, see: (d) Tormena, C. F.; Dias, L. C.; Rittner, R. J. *Phys. Chem. A* **2005**, *109*, 6077.
- (20) (a) Evans, D. A.; Chapman, K. T. *Tetrahedron Lett.* **1986**, 27, 5939. (b) Evans, D. A.; Chapman, K. T.; Carreira, E. M. *J. Am. Chem. Soc.* **1988**, *110*, 3560.
- (21) Frisch, M. J.; Trucks, G. W.; Schlegel, H. B.; Scuseria, G. E.; Robb, M. A.; Cheeseman, J. R.; Scalmani, G.; Barone, V.; Mennucci, B.; Petersson, G. A.; Nakatsuji, H.; Caricato, M.; Li, X.; Hratchian, H. P.; Izmaylov, A. F.; Bloino, J.; Zheng, G.; Sonnenberg, J. L.; Hada, M.; Ehara, M.; Toyota, K.; Fukuda, R.; Hasegawa, J.; Ishida, M.; Nakajima, T.; Honda, Y.; Kitao, O.; Nakai, H.; Vreven, T.; Montgomery, Jr., J. A.; Peralta, J. E.; Ogliaro, F.; Bearpark, M.; Heyd, J. J.; Brothers, E.; Kudin, K. N.; Staroverov, V. N.; Kobayashi, R.; Normand, J.; Raghavachari, K.; Rendell, A.; Burant, J. C.; Iyengar, S. S.; Tomasi, J.; Cossi, M.; Rega, N.; Millam, N. J.; Klene, M.; Knox, J. E.; Cross, J. B.; Bakken, V.; Adamo, C.; Jaramillo, J.; Gomperts, R.; Stratmann, R. E.; Yazyev, O.; Austin, A. J.; Cammi, R.; Pomelli, C.; Ochterski, J. W.; Martin, R. L.; Morokuma, K.; Zakrzewski, V. G.; Voth, G. A.; Salvador, P.; Dannenberg, J. J.; Dapprich, S.; Daniels, A. D.; Farkas, Ö.; Foresman, J. B.; Ortiz, J. V.; Cioslowski, J.; Fox, D. J. *Gaussian 09, Revision B.1*; Gaussian, Inc.: Wallingford, CT, 2009.
- (22) Scalmani, G.; Frisch, M. J. *J. Chem. Phys.* **2010**, *132*, 113110.
- (23) Marenich, A. V.; Cramer, C. J.; Truhlar, D. G. *J. Chem. Phys. B* **2009**, *113*, 6378.
- (24) B3LYP hybrid functional: (a) Lee, C.; Yang, W.; Parr, R. G. *Phys. Rev. B* **1988**, *37*, 785. (b) Becke, A. D. *Phys. Rev. A* **1988**, *38*, 3098. (c) Becke, A. D. *J. Chem. Phys.* **1993**, *98*, 5648.
- (25) Barone, V.; Cossi, M. *J. Phys. Chem. A* **1998**, *102*, 1995.
- (26) Glendening, E. D.; Badenhoop, J. K.; Reed, A. E.; Carpenter, J. E.; Bohmann, J. A.; Morales, C. M.; Weinhold, F. *NBO 5.9*; Theoretical Chemistry Institute, University of Wisconsin: Madison, WI, 2009; <http://www.chem.wisc.edu/~nbo5>.
- (27) (a) Wang, S. C.; Beal, P. A.; Tantillo, D. J. *J. Comput. Chem.* **2010**, *31*, 721. (b) Bond, D. J. *Org. Chem.* **2007**, *72*, 7313.
- (28) The effects of dipole minimization have also been used to explain the selectivity of aldol reactions involving oxazolidinones; see ref 1a. We can also see the effect of dipole minimization in aldol and Baeyer–Villiger reaction between fluor atoms. (a) Itoh, Y.; Yamanaka, M.; Mikami, K. *Org. Lett.* **2003**, *5*, 4807. (b) Itoh, Y.; Yamanaka, M.; Mikami, K. *Org. Lett.* **2003**, *5*, 4803.